Dissertation

The Influence of Bile Acids on Thrombin Generation in Cholestatic Liver Injury - In vitro Studies and Translational Aspects

submitted by

Dr.med.univ. Theresa Bauer

for the Academic Degree of

Doctor of Medical Science

(Dr. scient. med.)

at the

Medical University of Graz

Department of Pediatrics and Adolescent Medicine

under the Supervision of

Priv.-Doz. Dr. scient.med. Axel Schlagenhauf

Graz, 20. June 2023

Declaration

I hereby declare that this thesis is my own original work and that I have fully acknowledged by name all of those individuals and organisations that have contributed to the research for this thesis. Due acknowledgement has been made in the text to all other material used. Throughout this thesis and in all related publications I followed the guidelines of "Good Scientific Practice and Ombuds Committee at the Medical University of Graz".

Graz,20 June 2023 *Theresa Bauer eh*

Disclosures

Parts of this thesis have been published in the following article:

Greimel T, Jahnel J, Pohl S, Strini T, Tischitz M, Meier-Allard N, et al. Bile acid-induced tissue factor activity in hepatocytes correlates with activation of farnesoid X receptor. Lab Invest. 2021;101(10):1394-402.

List of all co-authors and their institutions:

Theresa Greimel[1], Jörg Jahnel[1], Sina Pohl[1], Tanja Strini[1], Martin Tischitz[1], Nathalie Meier-Allard[2], Sandra Holasek[2], Katharina Meinel[1], Victor Aguiriano-Moser[1], Joachim Zobel[1], Harald Haidl[1], Siegfried Gallistl[1], Katrin Panzitt[3], Martin Wagner[3], Axel Schlagenhauf[1]

[1] Division of General Paediatrics, Department of Paediatrics and Adolescent Medicine
[2] Division of Immunology and Pathophysiology, Otto Loewi Research Center
[3] Division of Gastroenterology and Hepatology, Department of Internal Medicine

– all Medical University Graz, Graz, Austria

I confirm that all co-authors have explicitly agreed to the use of their data in this thesis and that I have obtained permission to reproduce all figures and tables published in Greimel et al. from the respective copyright holder (Springer Nature).

Acknowledgements

I would like to express my sincere gratitude to the following persons/institutions:

My first supervisor, Axel Schlagenhauf, for his continuing scientific and personal support, for being accessible even on weekends and holidays, for his guidance and motivation skills and his great knowledge. Thank you for the opportunity to work with you.

My second supervisor, Jörg Jahnel, for his leadership and motivation in tough times, for bringing in new ideas and for the establishement of our research group.

My third supervisor, Martin Wagner, for his profound knowledge, his always helpful insights and constructive criticism and for giving this work the necessary changes of direction.

Sina Pohl, Tanja Strini and Martin Tischitz, for putting so much time and effort in this study, for being patient with me and my pipetting skills and for being great friends.

Nathalie Meier-Allard, for her support and especially her patience when explaining and showing the same things a thousand times to me.

Sandra Holasek, for the great collaboration between our institutes.

The Doctoral School of Molecular Medicine and Inflammation, for the opportunity to write this thesis.

Katharina Meinel, for her friendship, her trust and for never rolling her eyes at me.

My parents, Alexandra and Christian, and my sister, Christina, for their continuing love and support in good and bad days. Without you, I would not be where I am right now.

Sebastian, for supporting me in every way possible. You helped me to find myself.

Florentina, for being my world. I love you to the moon and back.

Table of contents

Abbreviations

6-ECDCA	6α-ethyl-chenodeoxycholic acid
aBA	atypical bile acids
ASBT	apical sodium dependent bile salt transporter
Ac-DEVD-pNA	acetyl-Asp-Glu-Val- Asp p-nitroanilide
ANIT	α-naphtylisothiocyanate
APC	activated protein C
aPTT	activated partial thromboplastin time
ASM	acid sphingomyelinase
AT	antithrombin
BA	bile acids
BSEP	bile salt export pump
CA	cholic acid
CAT	calibrated automated thrombography
Ca^{++}	calcium-ions
CDCA	chenodeoxycholic acid
CFTR	cystic fibrosis transmembrane regulator
CTI	corn trypsin inhibitor
CYP27A1	sterol-27-hydroxylase
CYP7A1	cholesterol 7α-hydroxylase
CYP7B1	oxysterol 7α-hydroxylase
CYP8B1	sterol 12α-hydroxylase
DAPI	4′,6-diamidino-2-phenylindole
DCA	deoxycholic acid
DMEM	Dulbecco's Modified Eagle's Medium
DMSO	dimethyl sulfoxide
EHC	enterohepatic circulation
ELISA	enzyme-linked immunobsorbent assay
EPCR	endothelial cell protein C receptor
ER	endoplasmatic reticulum
ETP	endogenous thrombin potential
FXR	farnesoid receptor X
FI	Factor I
FIa	activated Factor I
FII	Factor II
FIIa	activated Factor II

FIII	Factor III
FIIIa	activated Factor III
FV	Factor V
FVa	activated Factor V
FVII	Factor VII
FVIIa	activated Factor VII
FVIII	Factor VIII
FVIIIa	activated Factor VIII
FIX	Factor IX
FIXa	activated Factor IX
FX	Factor X
FXa	activated Factor X
FXI	Factor XI
FXIa	activated Factor XI
FXII	Factor XII
FXIIa	activated Factor XII
FXIII	Factor XIII
FXIIIa	activated FXIII
GAPDH	glyceraldehyde-3-phosphate dehydrogenase
GCDCA	glycochenodeoxycholic acid
GPIbα	gkycoprotein Ibα
GPIIb/IIIa	glycoprotein IIb/IIIa
HSD3B7	3β-hydroxy-Δ5-C27-steroid oxidoreductase
I-BABP	intestinal BA-binding protein
IRE1α	inositol-requiring enzyme 1α
LDH	lactate dehydrogenase
LCA	lithocolic acid
MDR1	multidrug-resistance-associated protein 1
mRNA	messenger ribonucleic acid
MRP2	multidrug resistance-associated protein 2
MRP3	multidrug-resistance-associated protein
MTT assay	3-[4,5-dimethylthiazole-2-yl]-2,5-diphenyltetrazolium bromide metabolic activity assay
norUDCA	24-norursodeoxycholic acid
NTCP	sodium taurocholate cotransporting polypeptide
OATPs	organic anion transporting proteins
OCA	obeticholic acid

OST- α	organic-solute-transporter α
OST- β	organic-solute-transporter β
PAR-1	protease activated receptor-1
PAR-4	protease activated receptor-4
PBC	primary biliary cholangitis
PBS	phosphate buffered saline
PDI	protein disulfide isomerase
PDGFB	platelet-derived growth factor beta
PL	phospholipids
pNA	p-nitroaniline
PS	phosphatidylserine
PSC	primary sclerosing cholangitis
PT	prothrombin time
qPCR	quantitative polymerase chain reaction
SHP	small heterodimer partner
TCA	taurocholic acid
TF	tissue factor
TFPI	tissue factor pathway inhibitor
TM	thrombomodulin
UDCA	ursodeoxycholic acid
UPR	unfolded protein response
vWF	von Willebrand Factor
WST	water soluble tetrazolium
XBP1	x-box binding protein 1

Table of figures

Table of tables

Abstract

Background and aims:

Besides their traditional metabolic functions, bile acids (BA) have been shown to affect intrahepatic coagulation processes. Elevated BA concentrations present in cholestatic liver disease seem to activate tissue factor (TF) decryption, resulting in intrahepatic thrombin generation. However, the precise process of TF decryption within the liver tissue and the contribution of farnesoid X receptor (FXR), a nuclear bile acid receptor, are still not understood. In this work, the impact of distinct BA on TF action and thrombin generation in hepatocytes were explored and linked to initiation of FXR-mediated signaling and apoptosis.

Methods:

HepG2 cells and primary human hepatocytes were incubated with various concentrations of chenodeoxycholic acid (CDCA), glycochenodeoxycholic acid (GCDCA), ursodeoxycholic acid (UCDA), the synthetic FXR agonist GW4064 or the synthetic FXR antagonist DY268 for 12 and 24 hours respectively. MTT tests were used to determine cell viability. The activity of TF was evaluated by generating factor Xa and assessing thrombin generation through calibrated automated thrombography. Quantitative polymerase chain reaction (qPCR) was used to determine FXR activation. Western blotting was used to determine TF protein levels and fluorescence microscopy of stained HepG2 cells to denote overexpression of TF. Cleaved caspase-3 and increased Annexin V binding were tested as apoptotic markers.

Results:

Enhanced thrombin production in tandem with increased TF activity was seen with CDCA and GW4064 and in primary hepatocytes also with GCDCA. UDCA did not show any effect. TF activity significantly decreased when FXR activation was inhibited with the antagonist DY268. qPCR revealed that only CDCA and GW4064 induced the upregulation of FXR targets in HepG2 cells. Western blotting and fluorescence microscopy revealed no upregulation of TF, implying that TF decryption rather than upregulation occurred. No evidence of apoptosis was detected.

Conclusion:

Long-term contact of liver cells with elevated levels of endogenous BA could cause a disproportionate stimulation of FXR, resulting in the decryption of TF regardless of the amphiphilic nature of BA. The influence of BA on TF initiation is related to its capacity to enter the cells and activate FXR. TF decryption occurs in the absence of apoptotic mechanisms.

Zusammenfassung

Hintergrund und Zielsetzung:

Neben ihrer ursprünglich beschriebenen metabolischen Funktion spielen Gallensäuren (GS) eine Rolle bei der Blutgerinnung. Erhöhte GS Konzentrationen bei cholestatischen Lebererkrankungen scheinen die Blutgerinnung zu beeinflussen, indem sie Tissue Factor (TF) aktivieren, was zu vermehrter Thrombingeneration führt. Allerdings ist weder der genaue Mechanismus der TF Aktivierung innerhalb des Leberparenchyms, noch die Rolle von Farnesoid X Rezeptor (FXR), einem Kernrezeptor der Gallensäuren, beleuchtet. In dieser Arbeit wurde der Einfluss von verschiedenen Gallensäuren auf die TF Aktivität und die Thrombin Generation in Hepatozyten untersucht und die beobachteten Effekte mit FXR ahängigen Signalwegen und Apoptose korreliert.

Methoden:

HepG2 Zellen und primäre humane Hepatozyten wurden mit verschiedenen Konzentrationen von Chenodeoxycholsäure (CDCA), Glykochenodeoxycholsäure (GCDCA), Ursodeoxycholsäure (UDCA), mit dem synthetischen FXR-Agonisten GW4064 oder mit dem synthetischen FXR-Antagonisten DY268 für 12 bzw. 24 Stunden inkubiert. Die Zellviabilität wurde mit MTT Tests überprüft. Die TF Aktivität wurde mittels Faktor Xa Generation überprüft und die Thrombingeneration mittels kalibrierter automatisierter Thrombographie gemessen. Quantitative Polymerase Kettenreaktion (qPCR) wurde verwendet um die FXR Aktivierung zu bestimmen. Die TF Protein-Level wurden mittels Western Blot bestimmt und Fluoreszenzmikroskopie von gefärbten HepG2 Zellen wurde verwendet um eine etwaige Hochregulation von TF zu erkennen. Gespaltene Caspase-3 und Annexin V Bindung wurden als Apoptose-Marker herangezogen.

Ergebnisse:

Vermehrte TF Aktivität und Thrombingeneration wurden mit CDCA und GW4064 und in primären Hepatozyten auch mit GCDCA beobachtet. UDCA zeigte keine Effekte. Bei Inhibierung der FXR Aktivität durch den FXR-Antagonisten DY268, wurde eine deutlich verminderte TF Aktivität beobachtet. In der qPCR zeigte sich eine Hochregulierung der FXR-Zielgene nur mit CDCA und GW4064. In der Western Blot Analyse, sowie in der Fluoreszenzmikroskopie zeigte sich keine vermehrte TF Expression, was für eine TF-„Decryption“ statt Hochregulierung spricht. Es wurden keine apoptotischen Effekte beobachtet.

Schlussfolgerung:

Eine Langzeit-Exposition von Hepatozyten mit per se unschädlichen GS könnte zu intrazellulärer FXR-Überstimulierung führen. Die dadurch bewirkte TF Aktivierung ist unabhängig von den amphiphilen Eigenschaften der GS. Die Effekte der GS auf die TF Aktivierung korrelieren mit der Fähigkeit der GS, in die Zellen aufgenommen zu werden und FXR zu aktivieren. Die TF Aktivierung findet unabhängig von Apoptose-Mechanismen statt.

1 Introduction

1.1 Bile acids

Bile acids (BA) are soluble, amphiphatic molecules that are formed from cholesterol. One can distinguish primary BA, which are synthesized in the liver and secondary BA, which are formed by the action of bacterial enzymes in the small intestine. The most common BA in humans are the primary BA cholic acid (CA) and chenodeoxycholic acid (CDCA) and the secondary BA deoxycholic acid (DCA) and lithocholic acid (LCA). Ursodeoxycholic acid (UDCA) is a secondary BA which exists only in trace amounts in humans (1, 2).

In humans, physiological serum BA concentrations range from 2 µM (basal) to 10 µM (postprandial), while bile acid levels in portal vein plasma range from 20-50µM and may reach up to 100 µM postprandial. In human hepatocytes BA concentration is estimated to be less than 50 µM. In the bile ducts and the biliary tree BA concentration rises up to milimolar concentrations (3).

BA have many important physiological functions. By emulsifying dietary lipids and fat-soluble vitamins (vitamin A, D, E, K) they promote lipid absorption in the small intestine. By solubilizing cholesterol molecules with phospholipids and excreting them in mixed micelles, they facilitate elimination of cholesterol from the hepatocytes, excretion in the biliary tract and ultimately fecal elimination of cholesterol (1, 4). Since BA are effluxed from hepatocytes into biliary canaliculi, they stimulate bile flow via osmotic activity (4). Another function of BA is secretion of biliary phospholipids into bile. At higher phospholipid concentrations in bile, mixed micelles are formed which protect the bile duct epithelium from damage (1, 4).

Apart from their well-known digestive functions, BA also have receptor-mediated hormone-like functions and regulate for example lipid, glucose, vitamin A, and glucocorticoid metabolism (5-8).

1.1.1 Enterohepatic circulation

Approximately only 5% of BA in the human body undergo fecal elimination and are consequently replaced by de-novo synthesis in the liver (about 0.2 to 0.6g per day) (1, 9).

The majority of BA circulate between the liver and the small intestine between 4-12 times a day 4 (9), undergoing the so-called enterohepatic circulation (EHC). EHC ensures optimal concentrations of each BA in the BA pool. Conjugated BA are secreted from the hepatocytes into bile and pooled in the gallbladder. Postprandial contraction of the gallbladder leads to secretion of BA into the small intestine, where 95% of BA are actively reabsorped in the small intestine and return to the liver via portal venous blood. A spill-over of BA into peripheral circulation occurs, which can be measured in the plasma. Only a small amount of BA pass to the colon and become passively reabsorbed (2).

1.1.2 Primary BA formation

In BA synthesis, a “classical” pathway can be distinguished from an “alternative” or “acidic” pathway. Approximately 75% of human BA are formed via classical pathway, whereby cholesterol is hydroxylated to 7α-hydroxycholesterol by cholesterol 7α-hydroxylase (CYP7A1). CYP7A1 is a cytochrome P450 enzymes and by its action the rate limiting step in BA formation (10, 11). In the alternative pathway, cholesterol is hydroxylated by sterol-27-hydroxylase (CYP27A1), creating intermediate products that are subsequently hydroxylated by oxysterol 7α-hydroxylase (CYP7B1) (11). In both, the classical and the alternative pathway, 3β-hydroxy-Δ5-C27-steroid oxidoreductase (HSD3B7) modifies the sterol ring; its products can now undergo two different pathways, ultimately leading to formation of either CA or CDCA: C12-hydroxylation of HSD3B7 products by sterol 12α-hydroxylase (CYP8B1), leads to generation of CA; without C12-hydroxylation, CDCA is formed (10, 11). Thus, the action of CYP8B1 determines the CA/CDCA ratio, which may be used as a biomarker in cholestatic liver diseases (12, 13).

Before excretion from hepatocytes, primary BA are conjugated either to taurine or glycine, facilitating higher concentrations of BA in bile and the small intestine as well as efficient re-uptake in hepatocytes (2, 4, 14). In adults, most BA are conjugated with glycine, whilst in neonates, taurine is predominant (1, 15).

1.1.3 Secondary BA formation

Secondary BA are formed in the colon via action of anaerobic bacteria. By C7-dehydroxylation transformation of CA to DCA and CDCA to LCA occurs (2). UDCA is formed by by bacterial 7β-epimerization of CDCA and characterized by being less hydrophobic than other BA (16).

After absorption in the terminal ileum of the small intestine and re-uptake in the liver, secondary BA are conjugated with glycine or taurine same as primary BA. While DCA enters the EHC together with CA and CDCA, the highly cytotoxic LCA is conjugated twice during hepatic transportation, excreted into bile and rapidly eliminated from the body instead of being efficiently absorbed in the small intestine. In total, LCA accounts only for about 5% of the BA pool (2).

1.1.4 BA transporters

BA circulation within the EHC relies on BA secretion and uptake in hepatocytes, cholangiocytes and enterocytes. Those processes are tightly regulated by several transporters.

1.1.4.1 Hepatocyte transporters

The most important BA-uptake receptor is sodium-taurocholate cotransporter (NTCP), which regulates the uptake of conjugated BA into the basolateral hepatocytes from portal venous blood. Sodium-independent organic anion transporting proteins (OATPs) transport conjugated as well as unconjugated BA. The multidrug-resistance-associated protein 3 (MRP3) accounts for removing conjugated BA from the hepatocyte, mainly under cholestatic conditions (17, 18).

At the canalicular membrane of the hepatocyte, the ATP-dependent transporter bile salt export pump (BSEP) effluxes monovalent BA into bile and stimulates bile flow. BA, bilirubin and organic anions are excreted via multidrug resistance-associated protein 2 (MRP2). There are other transporting proteins, which are associated with BA but do not directly transport BA: Organic cations and cytotoxins are excreted via multidrug-resistance-associated protein 1 (MDR1), phospholipids via MDR3. AE2 excretes bicarbonate into bile and stimulates BA-independent bile flow and FIC1 is a translocating ATPase of aminophospholipids (17, 19).

1.1.4.2 Cholangiocyte transporters

There are three transporters located on the luminal membrane of the cholangiocyte, which are important for bile formation: Apical sodium dependent bile salt transporter (ASBT),

which takes up BA into the cholangiocyte, cystic fibrosis transmembrane regulator (CFTR), which is no BA transporter but enables chloride entry and exchanges $HCO3^-$ and AE2, facilitating bicarbonate secretion into bile. On the basolateral side of the cholangiocyte, MRP3, as well as organic-solute-transporter α and β (OSTα/OSTβ) are expressed and mediate the return BA to the portal circulation under cholestatic conditions (17, 20, 21).

1.1.4.3 Enterocyte transporters

ASBT is mainly responsible for the absorption of conjugated BA into the enterocyte in the terminal ileum. OATPs account for sodium-independent uptake of BA from the intestinal lumen. Unconjugated BA diffuse passively in the small and large intestine (22). The export of BA and return to portal-venous blood occurs on the basolateral membrane of the ileum and colon via MRP3 and OSTα/OSTβ (23). Intracellular intestinal BA transport occurs via intestinal BA-binding protein (I-BABP*)* (24).

1.1.4.4 Kidney transporters

ASBT is responsible for the uptake of BA from the glomerular filtrate in the proximal tubulus, while MRP2 transports divalent organic anion conjugates into urine and excretes BA into urine in cholestatic settings (17, 25).

1.1.5 BA receptors and intracellular signaling

Apart fom their classical roles in dietary lipid absorption, BA have been discovered to act as signaling molecules. They have been found to directly activate three nuclear receptors: Farnesoid X receptor (FXR), pregnane X receptor and vitamin D receptor (9). Also, they activate the nuclear receptor constitutive androstane receptor and the following membrane G protein-coupled receptors in the gastrointestinal tract: Takeda G protein receptor 5 and sphingosine-1-phosphate receptor 2 (26). In the following section, only FXR-dependent signaling will be described, since it was investigated in this research project.

1.1.5.1 FXR

FXR is not only expressed in the liver, but also in kidney, adrenal glands, intestinal and vascular tissue. Paradoxically, although being a nuclear receptor, it has also been found to

be expressed in human platelets (27). Unconjugated, as well as conjugated BA are able to act as FXR-ligands, with varying potential to activate FXR: CDCA is the most effective ligand, followed by LCA, DCA and CA, while UDCA as hydrophilic BA binds to but does not fully activate FXR (9, 28). Rather, UDCA has been shown to act FXR antagonistic (29). Synthethic FXR ligands include GW4064 and 6α-ethyl-chenodeoxycholic acid (6-ECDCA), amongst others (30).

FXR activation enables BA to regulate their own synthesis and metabolism (31). FXR activates the atypical nuclear receptor small heterodimer partner (SHP), which represses the expression of CYP7A1, thus inhibiting BA synthesis (32). Furthermore, BA exporter proteins in the hepatocytes as well as in the intestinal tract, such as BSEP and OSTα/OSTβ are upregulated, facilitating increased efflux of BA (33, 34).
In the small intestine FXR induces the expression of fibroblast growth factor (FGF)15 in mice and its human ortholog FGF19, which suppress CYP7A1 expression in the liver after reaching the hepatocytes through the portal circulation (32).

Apart from its role in BA metabolism, FXR has been found regulate lipid and glucose metabolism (35, 36). Additionally, it has been shown that FXR is required for liver regeneration (37) and that it is protective against the development of hepatocellular or cholangiocellular carcinoma in mice models (38, 39).

1.1.6 „Atypical“ BA

Besides the usual bile acids, various C-6-alpha and 6-beta hydroxylated BA, so-called “atypical” bile acids (aBA) have been identified in umbilical cord blood and amniotic fluid of neonates. During liver-development tri-hydroxylated BA are more abundant, since hydroxylation seems to be a hepato-protective mechanism (40, 41). Zöhrer et al. found that serum levels of the aBA tauro-ω-muricholic acid is elevated during early-onset sepsis in neonates (42). aBA have also been found in adults with cholestatic liver diseases, suggesting modifications of BA metabolism in fetal and adult cholestatic hepatocytes (40).

1.2 Cholestatic liver disease

Cholestasis – the impaired bile flow along the biliary daraige system – can result either from impaired bile formation in the hepatocyte or from dysfunctional bile secretion and/or bile flow (43). Disruption of BA formation leads to impaired clearance from hepatocytes and accumulation of biliary substances; consequently, infants present with cholestatic jaundice, hepatopathy and cirrhosis (44, 45). In obstructive cholestatic liver disease, the extrahepatic, as well as the small intrahepatic bile ducts are affected; hepatocellular cholestasis can be the result of (hereditary or acquired) transporter defects, cytoskeletal changes or it can be inflammation-induced (43, 46). Clinical features of cholestatic liver disease include jaundice, fatigue and in some cases pruritus. Laboratory findings might be abnormal ranges of alanine aminotransferase, aspartate aminotransferase, alkaline phosphatase, gamma glutamyl transpeptidase, and prothrombin time. Also, due to an accumulation of BA, their spill-over into systemic circulation results in elevated BA concentrations in the plasma. Apart from detailed family history and clinical examination, an ultrasound of the abdomen is useful, especially to rule out potential bile duct obstruction; a missing or abnormal gallbladder can hint to biliary atresia (47). An important step in the diagnostic workup of cholestatic liver disease is the percutaneous core needle liver biopsy, which can lead to the correct diagnosis in 90-95% of the cases (46, 48).

In infants, the most common cholestatic liver disease is biliary atresia (25-40%), which is fatal if untreated (49), followed by hereditary transporter defects, such as progressive familial intrahepatic cholestasis Type 1-6 and Alagille syndrome (46). In older children, chronic cholestatic liver diseases are seen; primary sclerosing cholangitis (PSC) can hereby be distinguished from autoimmune sclerosing cholangitis, which is also called primary sclerosing cholangitis/autoimmune hepatitis overlap (50).

In adults, progressive cholestatic liver diseases, such as PSC, secondary sclerosing cholangitis, primary biliary cholangitis (PBC) and intrahepatic cholestasis of pregnancy can be distinguished from cholestasis due to obstruction, e.g. gallstones malignant obstruction (51-54).

1.2.1 UDCA as treatment option

UDCA is frequently used as prescription drug in cholestatic liver diseases and diseases accompanied by liver impairement, like cystic fibrosis and drug induced liver injury (16, 55-

58). It is administered orally in an average dose of 10-15 mg/kg/day (3). It has been found to decelerate disease progression and improves values for serum biomarkers of hepatobiliary injury, at least in the short term (3, 29). There are four proposed modes of action for UDCA (3): Replacement of damaging endogenous bile acids (such as LCA), cytoprotective effects on hepatocytes and bile duct epithelial cells, immunomodulatory effects and stimulation of bile secretion. Also, by secretion of organic anions and bicarbonate, UDCA contributes to the stabilization of the so-called “biliary bicarbonate umbrella”, which is a molecular mechanism to shelter bile ducts (29).

Apart from abdominal pain, diarrhea, skin reactions and metabolic drug interactions, UDCA has a favourable safety profile if administered in moderate doses (59). Long-term use of high doses of UDCA seems to be associated with higher risks of adverse events in PSC therapy (60). In mouse models of biliary obstruction, UDCA was shown to aggravate bile infarcts and hepatocyte necroses through its choleretic effects (61).

1.2.2 BA-analoga as novel therapies

A novel treatment option for cholestatic liver disease is 24-norursodeoxycholic acid (norUDCA), whcih is a C_{23} homologue of UDCA. Compared to UDCA, norUDCA ameliorated liver injury and exhibited less toxicity in animal models of cholestasis (62). Zhu et al. recently discovered immune-modulatory effects of norUDCA, by reduction of CD8 T-cells (63). Also, in phase II studies in humans, norUDCA proved effective in counteracting cholestasis, hepatic inflammation and fibrosis, significantly reduced AP levels compared to placebo and exhibited a favourable safety profile (64, 65).

Another BA-derived new therapeutic agent is obeticholic acid (OCA), which is a semi-synthetic 6-ethyl analogue of CDCA. It is a potent FXR agonist, thereby influencing BA synthesis and metabolism (29, 66). OCA has been approved as second-line add-on therapy in adult PBC (alongside UDCA) and has been shown to reduce serum alkaline phosphatase levels in adult PSC patients (67). The most common side effect was described to be dose-dependent pruritus (66).

1.3 Coagulation

The formation of a stable clot after vessel injury is the result of several complex interactions on a molecular and cellular basis. During the last years, changes of paradigms were noted as the widely known model of the “coagulation cascade” was substituted by a cell-based model. Generally, blood coagulation can be separated into primary haemostasis (platelet action resulting in an unstable clot) and secondary haemostasis (plasma protein action as well as platelet action resulting in the formation of a stable fibrin clot). After formation of the stable clot the fibrinolytic system is activated to ensure physiological balance between thrombus formation and disintegration. If this homeostasis is disturbed, bleeding tendencies or thrombotic events might be the result.

1.3.1 Primary haemostasis

Primary haemostasis can be summarised in three steps: Platelet adhesion, activation and aggregation (68).

Usually platelets do not interact with the endothelial vessel wall. However, upon tissue damage, the subendothelial extracellular matrix is exposed to the blood stream, allowing platelets to come in contact with adhesive molecules like collagen and von Willebrand factor (vWF), acting as platelet ligands (69). There are several mechanisms upon which platelet adhesion to the vessel wall is ensured: Firstly, platelets bind to collagen, fibronectin and laminin via integrins such as glycoprotein IIb/IIIa (GPIIb/IIIa) in vessels with low blood stream like veins. Secondly, at the site of higher blood stream like in arterioles, platelets interact with vWF via platelet surface receptor X (68-70).

vWF is stored in α-granules of platelets as well as in Weibel-Palade bodies of endothelials cells and secreted in the blood stream periodically from the latter. When vessel damage occurs, circulating vWF rapidly binds to exposed collagen and becomes immobilized, facilitating binding to platelet GPIbα (71). Thus, vWF acts as a “fishing rod” for platelets.

Upon binding to extracellular matrix proteins, platelets become activated, denoted by conformational changes. Amongst other things, activation of platelets leads to secretion of their α-granules, thereby releasing platelet vWF and other platelet agonists, facilitating recruitment of more platelets and platelet-platelet-interaction like a “fishing net”. Also, GPIIb/IIIa is activated which binds fibrinogen in a calcium-dependent matter (69, 70, 72).

Consequently, primary haemostasis ends with the formation of an (unstable) wound closure with platelet aggregates.

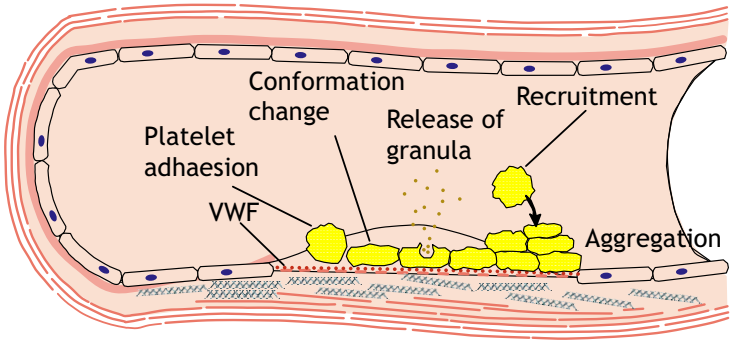

Figure 1. Depiction of platelet action in primary haemostasis (69).

1.3.2 Secondary haemostasis

1.3.2.1 The "coagulation cascade"

The widely known and accepted "cascade model" of coagulation has dominated the idea of coagulation for years. Originally developed in 1964, the model states that clotting is the result of a series of enzyme activations starting with the contact of blood with foreign surfaces. Table 1 denotes a list of coagulation factors, their original names and abbreviations.

Coagulation factor	Abbreviation (Factor/ activated factor)	Name (Factor / activated factor)
Factor I	FI / FIa	Fibrinogen / Fibrin
Factor II	FII / FIIa	Prothrombin / Thrombin
Factor III	FIII / FIIIa	Tissue factor; tissue thromboplastin
Factor V	FV / FVa	Proaccelerin
Factor VII	FVII / FVIIa	Stable factor
Factor VIII	FVIII / FVIIIa	Antihaemophilic factor A
Factor IX	FIX / FIXa	Antihaemophilic factor B; Christmas factor
Factor X	FX / FXa	Stuart Prower factor
Factor XI	FXI / FXIa	Plasma thromboplastin antecedent
Factor XII	FXII / FXIIa	Hageman factor
Factor XIII	FXIII / FXIIIa	Fibrin-stabilizing factor

Table 1. Coagulation factors, abbreviations and original names (73, 74).

The enzyme activation was believed to mimic a “cascade” as follows: Upon surface contact, FXII is converted to FXIIa, thereby activating FXI to FXIa, and so on, ultimately resulting in the conversion of fibrinogen (FI) to fibrin (FIa).

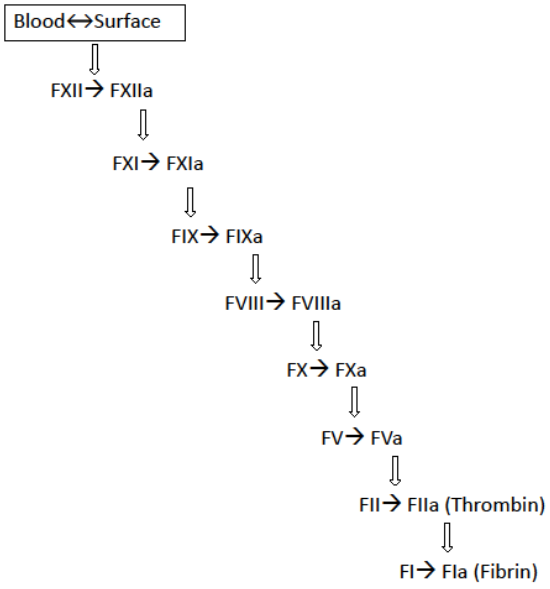

Figure 2. Earliest model of the „coagulation cascade“ (74)

Later on, the cascade was divided into an “extrinsic” and an “intrinsic”, as well as a “common” pathway. While the intrinsic pathway starts with contact activation, the extrinsic pathway was believed to be the result of tissue damage, thereby activating tissue factor (TF). TF is a transmembrane glycoproteine expressed on many cell surfaces. It is known as the “starting point” of coagulation and forms the TF/VIIa complex. Apart from its central function in haemostasis, TF is also known for its role in thrombosis, inflammation and even tumor growth (75).

Both pathways result in the activation of FX to FXa and ultimately merge in a “common pathway”, leading to the formation of thrombin and the conversion of fibrinogen to fibrin. Additionally, calcium-ions (Ca^{++}) are needed on a negatively charged surface (phospholipids; PL) to form enzymatic complexes (FVIIIa/FIXa and TF/FXa), ultimately activating FX and FII (73, 76).

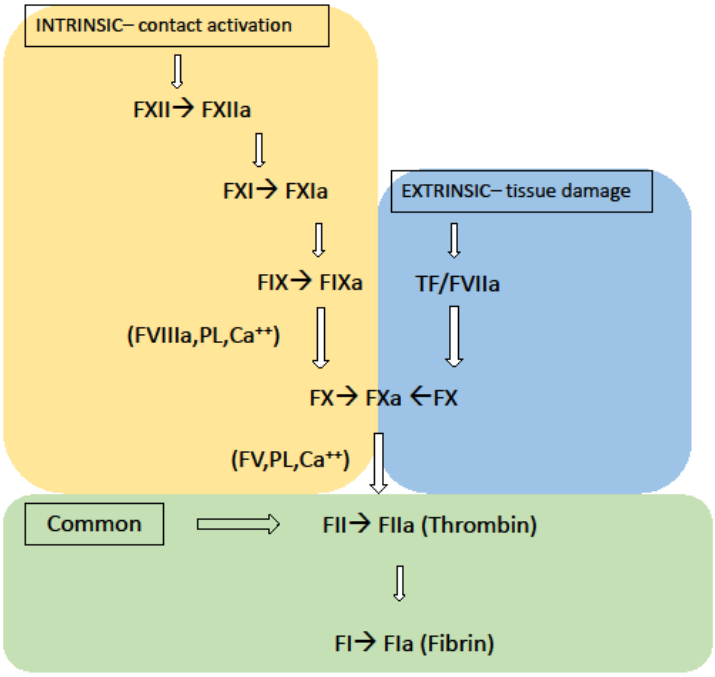

Figure 3. Expanded model of the “coagulation cascade” (73, 75, 76).
PL: phospholipids, Ca^{++}: Calcium.

In global coagulation assays, the “extrinsic” pathway is reflected in the prothrombin time (PT) and the “intrinsic” and common pathway in the activated partial thromboplastin time (aPTT) (77).

1.3.2.2 A cell based model of coagulation

Although the coagulation cascade explaines the interaction of coagulation fators and physico-chemical reactions in vitro, there are a few flaws of this model in vivo, for example the fact that haemophiliacs, who lack FVIII or FIX, still bleed, although they are supposed to have a normally working “extrinsic” pathway of the coagulation cascade, normally resulting in thrombin generation via formation of TF/VIIa complex. Furthermore, patients lacking components of the “intrinsic” pathway, e.g. FXII or pre-kallikrein, have indeed prolonged aPTTs but without any bleeding tendencies (77, 78).

During the last decade, a new explanation of coagulation in-vivo, the so-called “cell based model of coagulation” was developed (77). It was postulated that the cell surface on which coagulation takes place in vivo plays a critical role for the initiation, maintenance and smooth operation of haemostasis. However, no single cell type provides all necessary procoagulant complexes: Platelets are well equipped to generate large amounts of thrombin; however, they lack TF which is the only known physiological trigger of coagulation processes. On the other hand, TF bearing cells, such as monocytes or endothelial cells cannot produce enough thrombin to ensure sufficient clot formation and stabilization (78). Thus, generated FXa on a TF bearing cell via TF/FVIIa complex (“extrinsic pathway”) is not enough to provide effective haemostasis; FXa on a platelet surface, supported by the “intrinsic” FVIIa/VIXa complex is needed to ensure enough thrombin generation to form a stable clot (77, 79).
The cell based model of coagulation comprises three phases, Initiaton, amplification and propagation, which take part on various cell surfaces and overlap each other (80).

1.3.2.2.1 Initiation

The initiation phase can potentially start on every TF bearing cell, e.g monocytes, macrophages, activated endothelial cells or smooth muscle cells. An injury of the vessel enables contact of plasma with TF bearing cells and exposed TF binds to plasma FVII and forms the TF/VIIa complex which subsequently activates FX and FIX. Together with FVa, a small amount of thrombin is generated (81, 82).

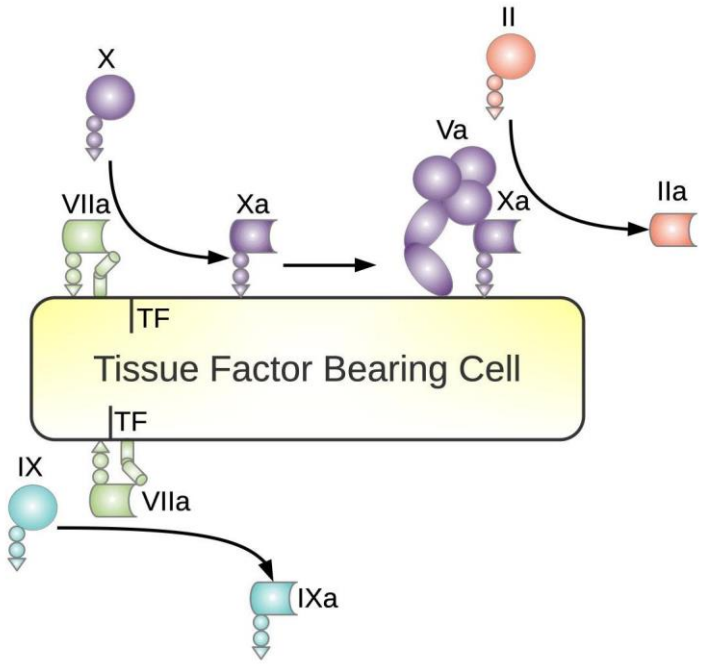

Figure 4. The initiation phase of the cell based model of coagulation (81).

1.3.2.2.2 Amplification

At the site of injury, platelets adhere to the extravascular matrix and are partially activated. During the amplification phase, the small amount of thrombin which was generated in the initiation phase fully activates platelets, which release partially activated FV from their alpha granules that is then fully activated by thrombin. Upon activation, the platelet plasma membrane changes and negatively charged PL, such as phosphatidylserine (PS) moves from the inner to the outer leaflet of the cell membrane, thus providing a procoagulant surface (83). Besides, the vWF/FVIII complex binds to platelets and FVIII is cleaved and activated by thrombin (84). Thus, at the end of the amplification phase, platelets and their cofactors FV and FVIII are activated to ensure extensive thrombin generation in the following third phase (85, 86).

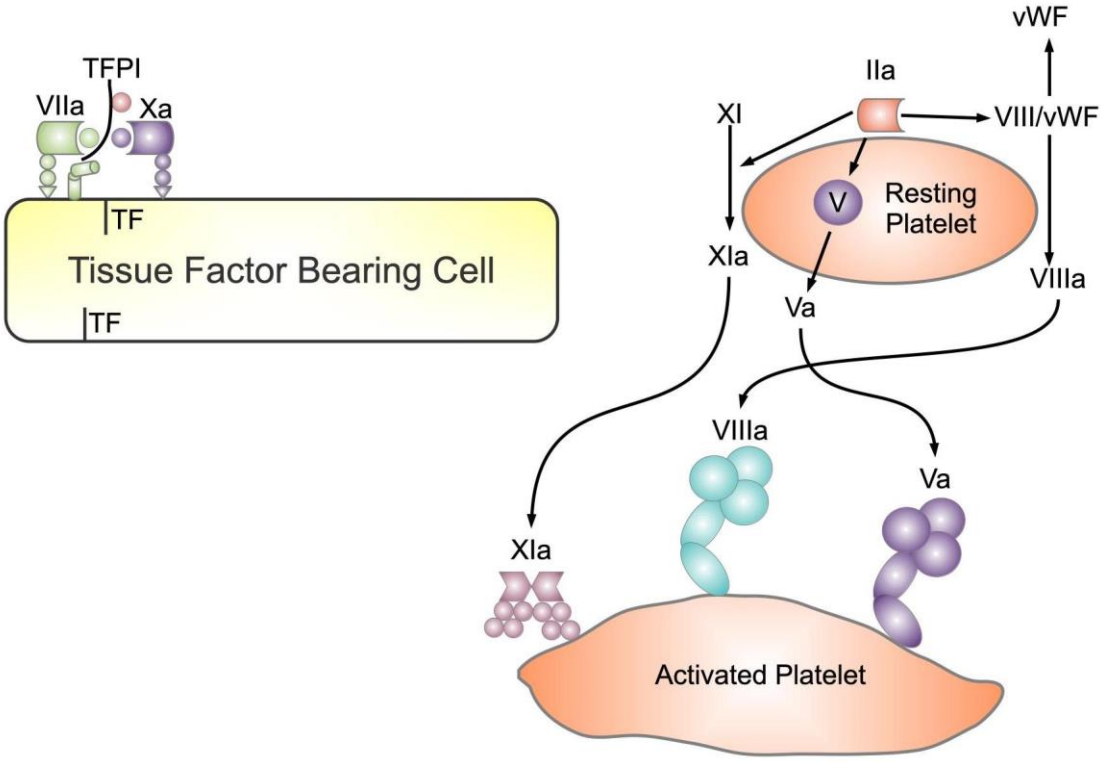

Figure 5. The amplification phase (81).

1.3.2.2.3 Propagation

To facilitate the so-called “thrombin-burst” – a large amount of thrombin, which is necessary to form a fibrin clot – the “tenase” (FVIIIa/IXa), as well as the “prothrombinase” (FXa/FVa) complex have to be formed on the platelet surface (81). There are two ways for FIXa to get into action: Firstly, FIXa reaches the platelet suface via diffusion after activation on the TF bearing cell during the initiation process. Secondly, plasma FXI binds to the platelet surface, where it is activated by thrombin and provides additional FIXa. The FVIIIa/FIXa complex activates FX, which subsequently binds to its cofactor FVa, ensuring the “thrombin burst” required for sufficient fibrin generation to stabilize the clot (81, 84).

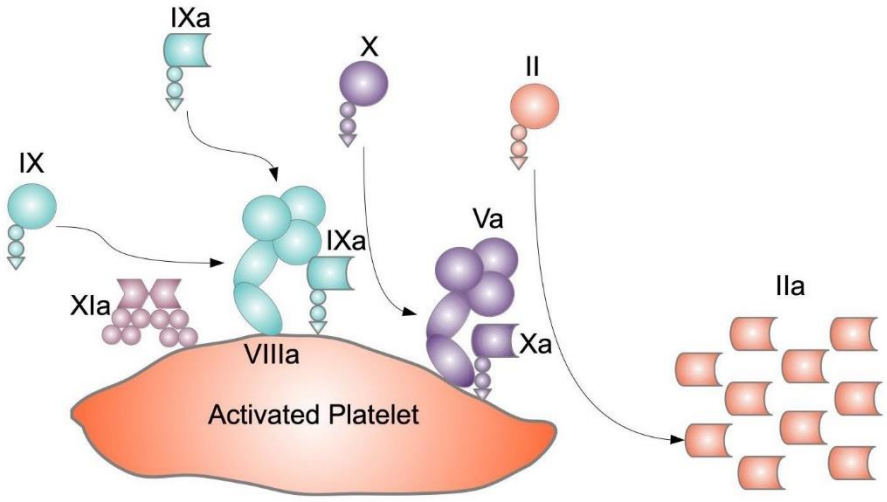

Figure 6. The propagation phase (81).

1.3.2.3 TF decryption

To prevent exuberant haemostatic action, TF is usually present on cell surfaces in an inactivated, encrypted state. In this conformational state TF is unable to activate Factor X. Upon decryption, coagulation mechanisms can start (87, 88). The proposed mechanism for TF decryption is an alteration in plasma membrane PL composition ("flip-flop effect"), leading to conformational changes of the TF/FVIIa complex, thereby being identified by its substrate FX. This flip-flop effect might be due to apoptotic mechanisms (89). Otherwise, tissue factor can be decripted by an increase in protein disulfide isomerase on the plasma membrane (90). Another proposed mechanism is TF decryption by acid sphingomyelinase (ASM), since acid sphingomyelin, which is a protein in the plasma cell membrane was found to keep TF in an encrypted state (91, 92)

1.3.3 Inhibition of blood coagulation

Clot formation is a tightly regulated process in order to limit its extent to the site of injury. To prevent extensive coagulation resulting in live threatening events such as thrombosis, inhibitors of the blood coagulation system are needed. There are three major players in the regulation of coagulation: Tissue factor pathway inhibitor (TFPI), antithrombin (AT) and

protein C. TFPI is mainly synthesized on microvascular endothelial cells (93) and exerts its regulatory function by directly inhibiting FX and the TF/VIIa complex (94). Also, activated platelets release platelet-derived TFPI, modulating TF action at the site of vessel injury (95). AT is synthesized in the liver; it can inhibit all procoagulant proteases but its main targets are thrombin, FXa and FXIa (96).

AT acts by binding to the active-site pocket of a coagulation protease, leading to conformational changes of AT, thereby trapping the coagulation protease and disrupting its catalytic function. In addition, a basic D-helix binds to therapeutic heparins on vascular endothelial cells, thereby reactivating coagulation proteases via conformational changes and imposing an important anticoagulant function (97).

Protein C is a plasma protein, which is synthesized in the liver (98). Via endothelial cell receptors thrombomodulin (TM) and endothelial cell protein C receptor (EPCR) protein C gets activated to activated protein C (APC) upon binding to thrombin. Together with its cofactors (protein S, FV, anionic PL and glycosphingolipids) APC irreversibly cleaves FVa and FVIIIa to their inactivated forms (99, 100).

1.3.4 The role of coagulation in cholestatic liver injury

Plasma flow from sinusoidal blood into the space of Disse is facilitated via fenestrated sinusoidal endothelial cells in the liver (101), enabling exchange of plasma proteins, e.g. coagulation factors. Consequently, the local microenvironment surrounding hepatocytes and cholangiocytes is susceptible to hemostatic action. In animal models of cholestatic liver injury fibrin deposits were found, hinting to local coagulation processes (102, 103).

However, the pathophysiological role of local coagulation activation (thrombin activity and platelet activation) relating to the progression of cholestatic liver diseases is unclear. Especially the role of platelets is controversial: Yoshida et al. stated that platelets *promote* biliary fibrosis in mice by producing platelet-derived growth factor beta (PDGFB), a mitogen that activates hepatic stellate cells (104). By contrast, Joshi et al. claimed that thrombin induced platelet activation *reduces* cholestatic liver injury and has hepatoprotective effects. In mouse models, they investigated the role of protease activated receptor-4 (PAR-4) and αIIbβ3 integrin on mouse platelets. Both represent pathways coupling coagulation to platelet activation. Mice that were unable to execute those pathways showed exacerbated biliary fibrosis, more widespread hepatocellular necrosis and liver fibrosis than controls (105). In a series of experiments Sullivan et al. demonstrated that TF-dependent thrombin generation

and protease activated receptor-1 (PAR-1) activation *contribute* to liver fibrosis induced by chronic cholestasis. They fed mice deficient in either TF or PAR-1 a diet containing α-naphtylisothicyanate (ANIT), a toxicant affecting bile duct epithelial cells, therefore simulating chronic cholestasis. TF deficiency, as well as PAR-1 deficiency led to a significant reduction of liver fibrosis in these mice. Also, TF and PAR-1 mRNA levels were increased in livers of patients with PBC and PSC (106). The discrepancies in these conducted in vitro studies might be due to the usage of several different mouse models (ANIT diet, bile duct ligation, Mdr2-knockout, etc.).

To date, the exact trigger of local coagulation in the liver it is not clear. Considering the physiology of blood coagulation, TF ought to be initiating coagulation processes. However, TF is present on hepatocytes in an encrypted form (75).

Sullivan et al. found that high levels of taurocholic acid (TCA) increase the procoagulant activity of TF in hepatocytes (107). In a subsequent study, they uncovered procoagulant activity of BA via direct activation of FX by interacting with a complex of recombinant TF and FVIIa (108). Thus, nontoxic BA could be involved in prompting intrahepatic coagulation in cholestatic liver diseases.

1.4 Aim of the study and scientific impact

The goal of this study was to evaluate the influence of specific BA on blood coagulation processes in hepatocytes. Based on this goal the following aims will be addressed:

- Aim 1: To test the hypothesis that long-term exposure of hepatocytes to various BA has a procoagulant effect via enhanced TF activity and thrombin generation.
    - In this aim, TF activity after incubation of HepG2 cells and primary human hepatocytes with various BA will be measured. Moreover, thrombin generation after incubation of hepatocytes with BA will be determined. Experiments will be performed after long-term exposure of the cells to BA (12 hours and 24 hours respectively).

- Aim 2: To test the hypothesis that procoagulant effects occur via TF decryption not by membrane interactions but by intracellular signaling involving the nuclear BA receptor FXR.
    - In this aim, FXR activation will be tested and correlated with the corresponding TF activity and thrombin generation. Negative control experiments will be performed with FXR antagonist DY268 and by measuring TF mRNA and protein levels and visualizing potential TF upregulation or redistribution.

- Additional aim: To rule out apoptotic mechanisms as cause for potential procoagulant effects.
    - In this aim, cell death will be investigated via determination of cell viability, cytotoxicity, Caspase-3 activity and Annexin V binding.

The activation of blood coagulation in cholestatic liver disease has been discussed, but the underlying mechanism has not been elucidated yet. By answering key questions concerning the impact of BA on local coagulation processes, this work will contribute to the knowledge of cholestasis and intrahepatic coagulation. Furthermore, the results of the present study might have future implications when targeting possible signaling pathways in the therapy of cholestatic liver diseases.

2 Materials and methods

2.1 Cell culture

2.1.1 Cell culture

Human hepatoma cells (HepG2 cells) alongside primary human hepatocytes were used for all experiments. HepG2 cells are characterized by high proliferation rates and epithelial-like morphology. Due to their unlimited life span and easy handling, HepG2 cells are common alternatives to the costly primary human hepatocytes (109).

Human HepG2 cells (originally acquired from CLS Cell Lines Service, Eppelheim, Germany, and tested for Short Tandem Repeat-verification before usage) were cultured in a special modification of DMEM (Dulbecco's Modified Eagle's Medium: 1g/l D-Glucose, L-Glutamine Pyruvate; GIBCO, Thermo Fisher Scientific, Waltham, MA, USA), with 10% Fetal Bovine Serum (GIBCO) and 1% Penicillin-Streptomycin (GIBCO) at 37°C and 5% CO^2 in 75 cm^2 tissue culture flasks with a concentration of 10^6 cells/mL. Split ratio was 1:4 to 1:6 every 3 to 4 days. For splitting, the medium was removed and the cells were washed twice with 8mL PBS (Phosphate Buffered Saline, GIBCO). 4mL of 0.05% Trypsin-EDTA (GIBCO) was added, followed by incubation at 37°C for 3 minutes. By tapping the flask, cells were dissolved and 4ml medium was added to stop the reaction with trypsin. The suspension was thoroughly mixed and centrifuged at 2500 rpm for 3 minutes. The pellet was then resuspended in 2mL medium and 10-18 mL medium (depending on the cell density) were added before counting. Cells were then brought to a concentration of $1x10^6$ cells/mL and incubated at 37°C. Prior to the experiments, cells were seeded in 6-well-plates and incubated at 37°C for 24 hours.

Frozen primary human hepatocytes from three different donors (5×10^6 cells/batch) as well as thawing, plating, and maintencance medium were acquired from Lonza (Walkersville, MD). Cryopreserved cells were thawed for 90-120s, moved into thawing medium, spun, and then transferred into plating medium. Viability and yield were evaluated using the Trypan blue exclusion technique. Cells were brought to a concentration of 1×10^6 cells/ml and seeded into 24-well plates coated with collagen (0.5×10^6 cells/well). Cells were incubated overnight (37°C, 5% CO^2), and the plating medium was replaced by maintenance medium.

2.2 Cell Treatment

BA and GW4064 were purchased from Sigma (St.Louis, MO, USA). HepG2 cells were treated with concentrations ranging from 100 to 600 μM of CDCA, GCDCA and UDCA and with concentrations ranging from 1 to 40μM of GW4064 and incubated in 6-well plates at 37°C for 12 hours, 24 hours, 48 hours and 72 hours respectively. Dimethyl sulfoxide (DMSO) was used as vehicle. After incubation, BA were removed from the cells prior to all further experiments. In additional experiments, HepG2 cells were treated with tunicamycin in concentrations ranging from 10 to 60 μM and incubated in 6-well plates at 37°C for 24 hours.

2.3 Cell viability and cytotoxicity assays

Cell viability was assessed via a commercial 3-[4,5-dimethylthiazole-2-yl]-2,5-diphenyltetrazolium bromide (MTT) metabolic activity assay (ATCC Bioproducts, Manassas, VA). The assay is based on the reduction of tetrazolium salts by metabolically active cells, which can be quantified by spectrophotometric means and is widely accepted as a way to examine cell proliferation. After harvesting, cells were resuspended at 1 x 106 per mL and plated, in triplicates, on a 96-well plate (100 μL) and incubated for 24 hours. Afterwards, 10 μL MTT reagent was added and incubated until purple precipitate was visible. After adding 100 μL of detergent reagent, the suspension was incubated at room temperature in the dark for 2 hours. The absorbance was recorded on a plate reader at 570 nm. Blank wells, containing medium only and DMSO served as controls.

Cytotoxicity was assessed via release of lactate dehydrogenase (LDH) using a commercial LDH-Cytotoxicity Assay Kit (Abcam, Cambridge, UK). Upon cell death, released LDH oxidizes lactate to generate NADH, which reacts with water soluble tetrazolium (WST) and generates a yellow color, which can be quantified on a plate reader. After harvesting and washing with culture medium, 100 μL (with 10 x 104 cells per well) were transferred to a 96-well plate. The assay was performed according to manufacturer's instructions, including test samples, background controls, low controls and high controls. Samples were incubated at 37°C and centrifuged at 600 x g for 10 minutes. The supernatant was then transferred in a 96-well plate (10 μL per well). 100 μL LDH reaction mix was added to each well and incubated for 30 minutes at room temperature. The absorbance of all controls and samples was measured on a plate reader at 450nm (reference wavelength 650 nm).

All measurements were performed in duplicates from three independent experimental replicates (N=6).

2.4 TF activity assay

HepG2 cells were seeded in 6-well plates (2 x 106 cells/well) and incubated for 24 hours with various BA. Primary human hepatocytes were seeded into 24-well plates (0.5 x 10^6 cells/well) and treated equally. After 24 hours HBSA buffer (137 mM NaCl, 538 mM KCl, 555 mM glucose, 10 mM HEPES, 0.1% BSA) was warmed up to 37°C. Factor X (Human; 150 nM, CoaChrom Diagnostica, Maria Enzersdorf, Austria) was prepared with 1707,2 µL HBSA and 36 µL calcium chloride (1 M). After incubation the supernatant was transferred into an Eppendorf vial and centrifuged with 600 rpm for 5 minutes. After dismissal of the medium, the pellet containing the non-adherent cell fraction was resuspended in 750 µL HBSA and transferred in the wells. 5 µL Factor VIIa (Novoseven; 150 nM, Novo Nordisk, Vienna, Austria) and 255 µL of Factor X mixture (as described above) was added to each well. The 6-well plate was incubated at 37°C. After 15 minutes incubation, 250 µL EDTA (5 mM; Sigma) was added to stop the reaction and the supernatant was centrifuged with 13.000 rpm for 5 minutes. For 24-well plates containing primary hepatocytes only half of the reaction mix was used.

Generated factor Xa was detected in triplicates in a 96-well plate, using a chromogenic substrate (Perfachrome FXa 8595; 0.667 mM, Enzyme Research Labs, South Bend, IN, USA) on a plate reader (Thermo Fisher Scientific). 120 µl of the reaction mix from the 6/24-well plate were combined with 20 µl of the chromogenic substrate. The absorbance increase at 405 nM corresponding to the FXa concentration was traced for 60 minutes (average slope). Factor Xa concentrations were calculated via external calibration with FXa.

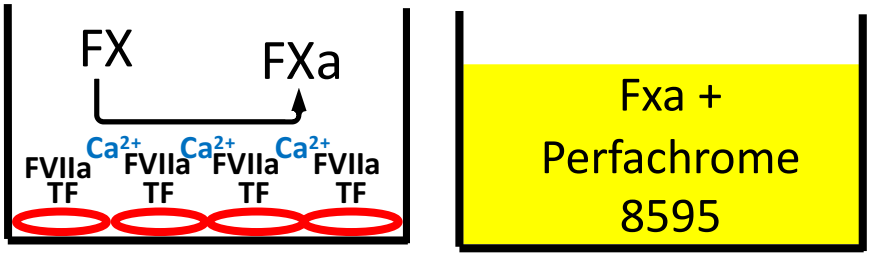

Figure 7. Schematic depiction of tissue factor activity assay.

2.5 Assessment of thrombin generation

The capability of a sample to create thrombin was evaluated by its total amount of thrombin action (endogenous thrombin potential, ETP), which was examined as the area under the curve, and the time before the thrombin discharge (lagtime). Calibrated Automated Thrombography (CAT) was utilized to determine thrombin generation as previously reported (110) without the inclusion of exogenous tissue factor. HepG2 cells were seeded into uncoated 96-well plates (0.1 x 10^6 cells/well, Immulon 2HB, Thermo Fisher Scientific) and incubated with the respective bile acids for 24h. After elimination of BA, 20 µl MP-reagent or calibrator (Thrombinoscope BV, Maastricht, Netherlands), and 80 µl in-house pooled plasma standard were added. Corn trypsin inhibitor (CTI, 0.1 mg/ml, Haematologic Technologies, Essex Junction, VT, USA) was added to prevent contact activation. Therefore, cell-derived TF was the only initiator for thrombin generation in the sample. Fluobuffer for monitoring thrombin generation curves contained 20 mM HEPES buffer (Thermo Fisher Scientific) and 60 mg/ml bovine serum albumin (Carl Roth, Karlsruhe, Germany) and was blended with calcium chloride solution (0.1 M final concentration, Merck, Darmstadt, Germany). The fluorogenic substrate Z-Gly-Gly-Arg-amino-methyl-coumarin (Bachem, Bubendorf, Switzerland) was solubilized in DMSO and added to the fluobuffer/calcium mixture before measurement (1.7 mg/ml final concentration). The measurement was initiated by automatic dispension of the fluobuffer/calcium mixture containing the fluorogenic substrate to each well (20 µl) and thrombin generation was tracked with the Thrombinoscope software (Thrombinoscope BV).

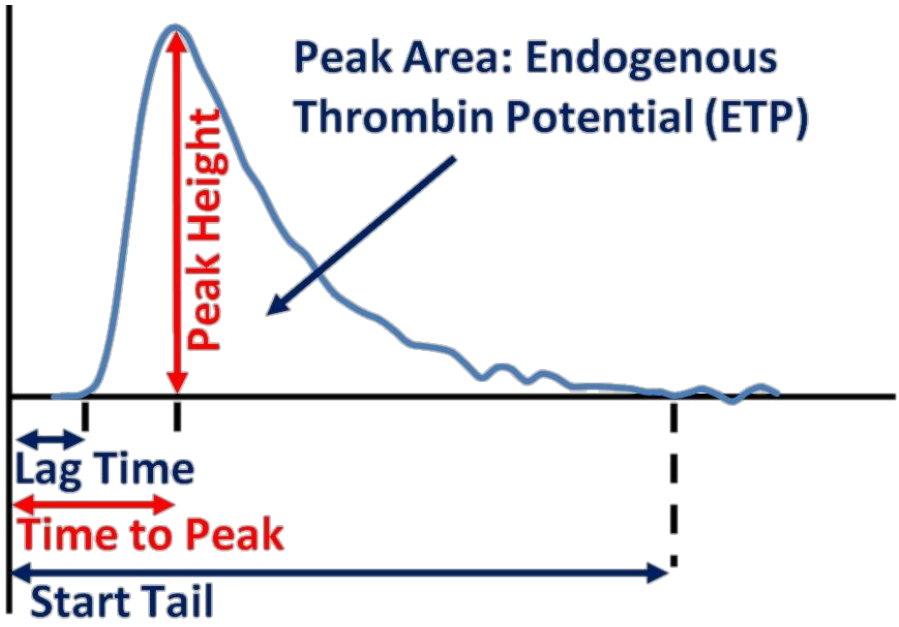

Figure 8. Parameters of thrombin generation measurements via calibrated automated thrombography.

2.6 Western blot analysis of TF protein levels

HepG2 cells were pre-treated with BA for a period of 24 hours. Subsequently, the cells were broken down in a solution containing 50 mM HEPES (from Sigma), 150 mM NaCl, 10% glycerol, 1% Triton X-100 (from Sigma) and an adjusted pH of 7.4 (lysis buffer). Additionally, Halt Protease and Phosphatase Inhibitor Cocktail (Thermo Fisher Scientific) was added to the lysis buffer in a ratio of 1:100. Protein content of the lysates was determined with a commercial BCA assay (Thermo Fisher Scientific). Ten micrograms of protein were resolved by sodium dodecyl sulfate polyacrylamide gel electrophoresis (SDS-Page) and transferred onto nitrocellulose membranes (Invitrogen, Thermo Fisher Scientific). Blotting buffer contained 25% methanol and 10% Tris buffered saline. Membrane was blocked with 5% blotting-grade blocker (Biorad). For immunodetection anti-tissue factor antibody (ab228968, Abcam, Cambridge, UK) and a mouse anti-rabbit IgG-HRP antibody (sc-2357, Santa Cruz Biotechnology, Dallas, TX) were used. A primary antibody for glyceraldehyde-3-phosphate dehydrogenase (GAPDH; Santa Cruz Biotechnology) was utilized as a reference and staining indicator. The blot strips were identified with a Molecular Imager Chemi DocTM XRST Imaging System (Bio-Rad). Quantification was done with 3 independent experimental replicates.

2.7 Caspase Activity Assay

HepG2 cells were treated with bile acids or GW4064 for a 24-hour period, following the established procedure. In addition, cells were exposed to 2 µM or 4 µM staurosporine as a positive control. After the treatment period, cell lysis was performed and the caspase activity was evaluated using a Caspase 3 Assay Kit (Sigma) designed for 96-well plates. This colorimetric test is based on the caspase 3-driven breakdown of the peptide substrate acetyl-Asp-Glu-Val-Asp p-nitroanilide (Ac-DEVD-pNA), which releases the p-nitroaniline (pNA) chromophore. The assay buffer and color-producing substrate were mixed with the cell lysates, incubated at 37°C for 10 hours, and the pNA release was measured at 405 nm. A pNA calibration curve was employed for quantification. Caspase 3 inhibitor (Ac-DEVD-CHO) was added to establish negative controls for each sample.

2.8 Quantitative polymerase chain reaction (qPCR)

HepG2 cells were incubated with various concentrations of bile acids for either 12 or 24 hours and then dissolved in RLT buffer (QIAGEN, Hilden, Germany). Cells that were only exposed to DMSO for the same time periods were employed as a control. RNA was extracted with the RNeasy Mini Kit (QIAGEN) as per the manufacturer's guidelines and the quantity was measured with a De Novix DS-11 spectrophotometer (Wilmington, DE, USA). Subsequently, cDNA was produced utilizing the Applied Biosystems High-Capacity RNA to cDNA Kit (Thermo Fisher) in a BioRad C1000 Touch Thermal Cycler (CFX96 Real-Time System) (Hercules, CA, USA). The relative gene expression of FXR-targets SHP, OST-α, OST-ß and TF were evaluated with ß-actin as the reference gene. The reactions were conducted in triplicates on 96-well-plates. Primers employed for this procedure were ACTB, Human (BIO-RAD Unique Assay ID: qHsaCED0036269); F3, Human (BIO-RAD Unique Assay ID: qHsaCED0036452); SHP (BIO-RAD, Custom Primer Pair Desalt 200R, fwd: GCTTCAATGCTGTCTGGAGTC, rev: CTTGGAGGCCTGGCACATC); OSTalpha (BIO-RAD, CustomPrimerPairDesalt200R, fwd: CAGATTGCTTGTTCGCCTCC, rev: ATTCGTGTCAGCACAGTCATTAG); OSTbeta (BIO-RAD, Custom Primer Pair Desalt 200R, fwd: CAGGAGCTGCTGGAAGAGAT, rev: GACCATGCTTATAATGACCACCA). SYBR Green fluorescent dye (Bio-Rad) was used for detection. 7.5 µl iQ™ SYBR Green Supermix (Bio-Rad), 2.75 µl RNAse-free water and 0.75 µl primer mix (250nM final concentration) were mixed in PCR tubes. 4 µl cDNA (1:10 dilution with nuclease-free water) of treated HepG2 cells or controls were transferred to 96-well plates and 11 µl master mix per each gene was added. The cDNA of the pooled RNA was also added to the master mix

for each gene to create a reverse transcription negative control (RT-), furthermore, no template controls were included in the experiment settings. The PCR conditions were executed on a CFX96 Touch Real-Time PCR Detection System (BIO-RAD): Initially 95°C for 3 min, then 40 cycles at 95°C for 15 sec and 60°C for 30 sec, followed by a melt curve with 60°C to 95°C (increase of 0.5°C/5sec). The data were normalized by the expression of β-actin and the relative gene expression was determined with the ΔΔCq method (111). ΔΔCq-values were normalized to 400 µM DMSO.

2.9 Fluorescence Microscopy

Cells were incubated with 600 µM of CDCA, GCDCA, UDCA, or 60 µM of GW4064 for a period of 24 hours. Subsequently, they were fixed in ice-cold ethanol for 5 minutes, washed twice in PBS (pH 7.2) and then exposed to an Alexa Fluor 546 conjugated TF antibody (sc-374441 AF546, Santa Cruz Biotechnology) (1:100 in 0.1% BSA) for 30 minutes. After this, cells were again washed with PBS and stained with 4′,6-diamidino-2-phenylindole (DAPI) (1 µg/ml) for 10 minutes. Finally, they were washed twice with PBS (pH 7.2) and then examined using fluorescence microscopy.

2.10 Flow cytometry analysis

HepG2 cells were incubated with respective bile acids or GW4064 for 24h and harvested using Accutase (Sigma; 5 min, room temperature). Cells were centrifuged, washed twice with PBS and resuspended in Annexin binding buffer (BD Pharmingen, 106 cells/ml). 100 µL of the suspension was stained with 5 µL or 10 µL FITC conjugated Annexin V (BD Pharmingen) and propidium iodide (Thermo Fisher) and incubated for 15 minutes in a dark place at room temperature. After incubation, 400 µL binding puffer was added. Cells were analysed within one hour using a Cytoflex S flow cytometer (Beckman Coulter). Gating strategy is depicted in Figure 20.

2.11 Statistics

The obtained parameters from different bile acid concentrations were tested against vehicle with ANOVA and Dunnett's post-hoc test using IBM SPSS Statistics 24.0 or Graphpad

Prism 9.3. P-values <0.005 were considered statistically significant. Data are presented as mean ± standard deviation (SD).

3 Results

3.1 Coagulation activation

3.1.1 TF activity assay

We found a clear time/dose dependency of TF action with CDCA in HepG2 cells:
TF activity went up slightly after 72h when 100 µM and 200 µM CDCA were applied (100 µM: 16.3±5.8 pM FXa/min; 200 µM: 11.6±4.7 pM FXa/min; vehicle: 5,9±3,1 pM FXa/min; $p<0.05$). With 400 and 600 µM CDCA, TF activity was significantly higher after 24h (400 µM: 44.2±34.8 pM FXa/min; 600 µM: 820±337 pM FXa/min; vehicle: 10.3±9.5 pM FXa/min; $p<0.001$) and continued to raise after 48h and 72h. At higher CDCA concentrations (600 and 1000 µM CDCA), TF activity began to increase after 15 minutes (600 µM: 11.4±0.5 pM FXa/min; 1000 µM: 23.9.±3.1 pM FXa/min; vehicle: 7.8±0.4 pM FXa/min; $p<0.05$) (Figure 9A).

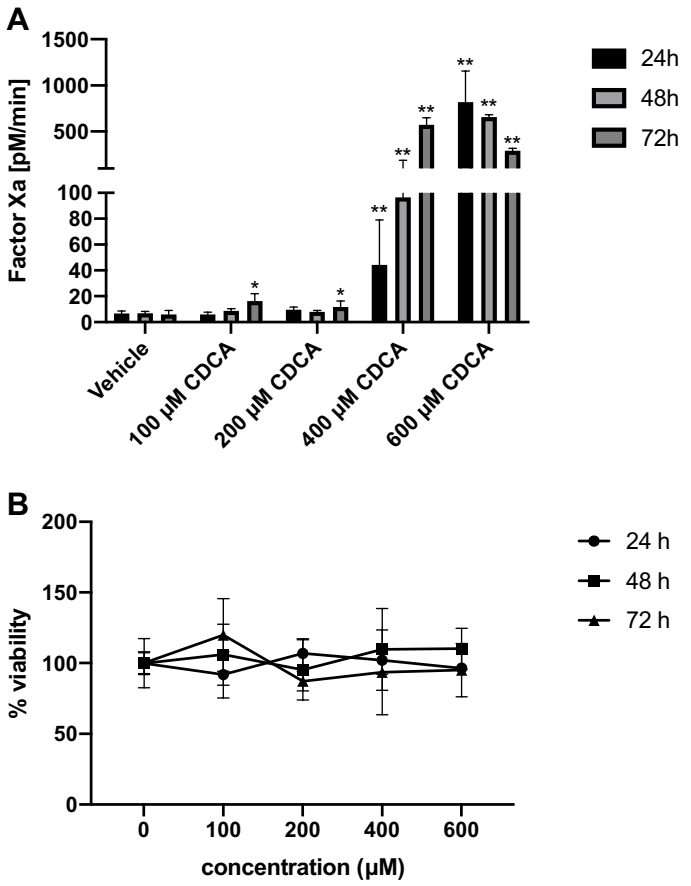

Figure 9. Increase of tissue factor (TF) activity after long-term exposure to CDCA in the absence of cell death (112).

(A) The effects of CDCA on the coagulation factor Xa (FXa) activity of HepG2 cells were evaluated. Cells were exposed to concentrations of 100, 200, 400, and 600µM of CDCA for 12h, 24h, 48h, and 72h with dimethyl sulfoxide (DMSO) used as the vehicle. The results were expressed as the mean ± standard deviation (SD) (N=6). Additionally, the viability of the cells was measured using the MTT assay **(B)** and expressed as the mean ± SD (N=6). Significant differences from the vehicle control were observed (*p<0.05; **p<0.001).

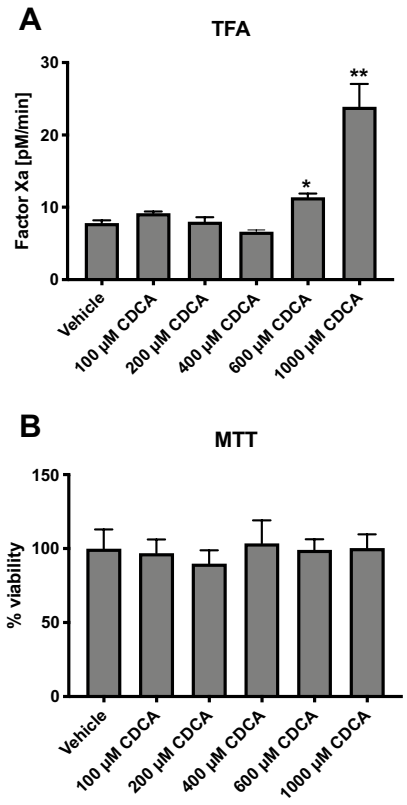

Figure 10. Tissue factor (TF) activity following incubation with several amounts of chenodeoxycholic acid (CDCA) for 15min (112).

The effect of CDCA on the activity of coagulation factor Xa (FXa) was measured in HepG2 cells. The cells were exposed to CDCA concentrations of 100, 200, 400, 600, and 1000µM with dimethyl sulfoxide (DMSO) as the vehicle, for 15 minutes. The results, based on six replicates, were expressed as the mean ± standard deviation **(A)**. Additionally, the viability of the cells was determined through the MTT assay **(B)**. The same concentrations of CDCA used for the FXa assay were used for the MTT assay. The percentage of cell viability was calculated and the results, based on six replicates, were expressed as the mean ± standard deviation. Significant differences from DMSO were indicated with $p<0.05$ and $p<0.001$.

GCDCA had no effect on TF activity in HepG2 cells in any of the experiments conducted and UDCA only increased TF activity at the highest concentration after 24 hours (600 µM: 52.9±1.3 pM FXa/min; vehicle: 14,5±1.2 pM FXa/min; $p<0.001$) (Figure 11A).

The synthetic agonist GW4064 caused a clear increase in TF activity over a period of 24 hours (Figure 11B). A difference in TF activity was already seen at low doses (5 µM: 40,2±18,35 pM FXa/min; vehicle: 12,6±4,3 pM FXa/min).

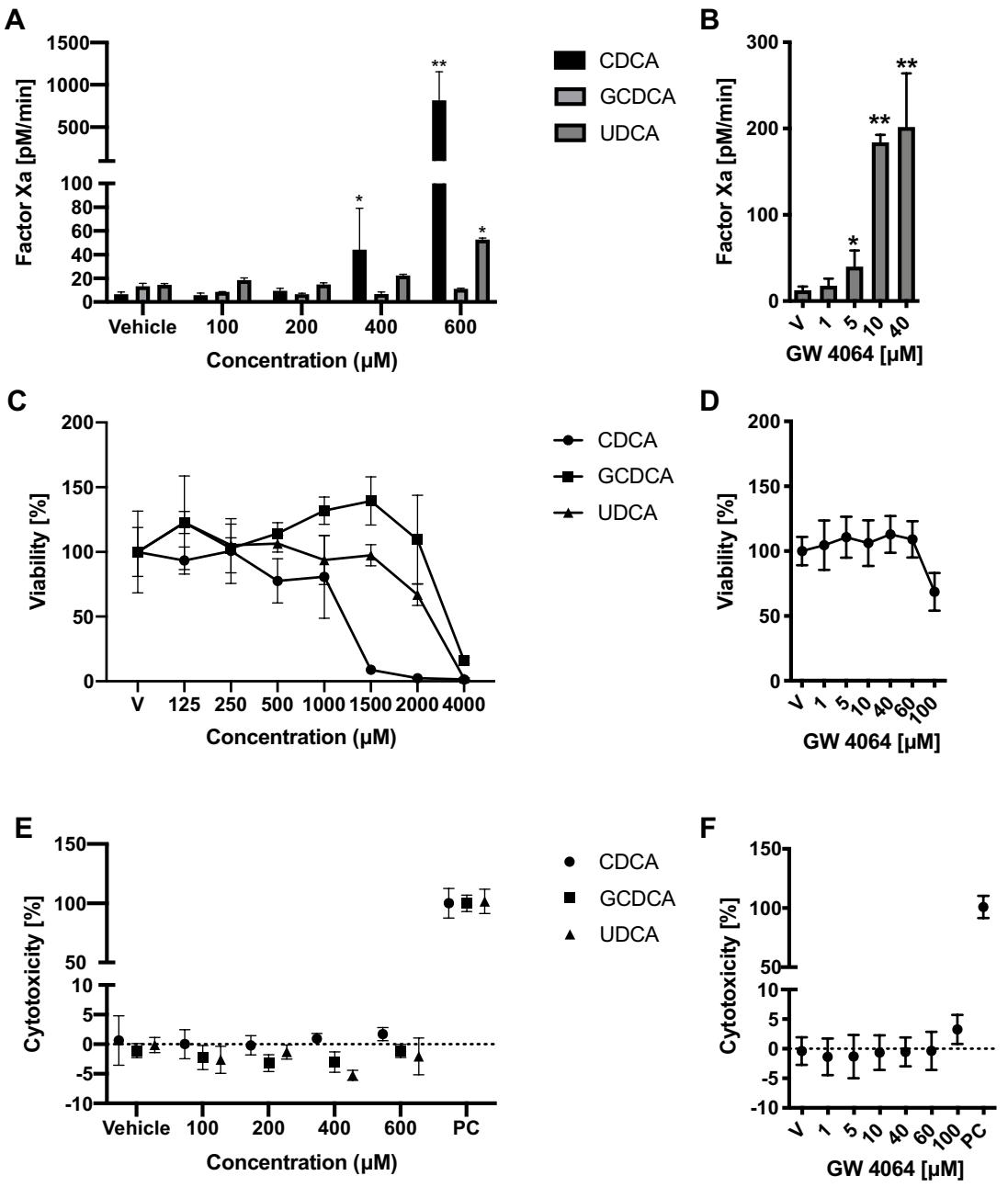

Figure 11. The effects of various bile acids or GW4064 on tissue factor (TF) activity, cell life, and toxicity (112).

HepG2 cells were tested for their level of coagulation factor Xa (FXa) activity after being exposed to CDCA, GCDCA, UCDA **(A)**, and GW4064 **(B)** for 24h. The concentrations used were from 100-600 μM for CDCA, GCDCA, and UCDA and from 1-40 μM for GW4064. As a control, dimethyl sulfoxide was also used. The results of the FXa activity test were augmented by an MTT assay **(C/D)** and cytotoxicity assay **(E/F)**. The MTT assay showed that with CDCA, GCDCA, and UDCA, the cells remained viable within the concentration ranges employed for TF activity assays. The cytotoxicity assay showed that there was no observable LDH release within the same concentration ranges. PC: positive control consisting of lysed cells. * $p<0.05$ for difference from vehicle; ** $p<0.001$ for difference from vehicle.

After 24 hours of incubation with the FXR inhibitor DY 268 (10 µM), no change in TF activity was observed with CDCA (Fig. 12A). Conversely, TF activity after 24 hours of exposure to GW4064 was significantly diminished in the presence of DY 268 (Fig. 12C). Neither CDCA/GW4064 nor DY 268 had any effect on cell viability in the used concentrations (Fig. 12 B/D).

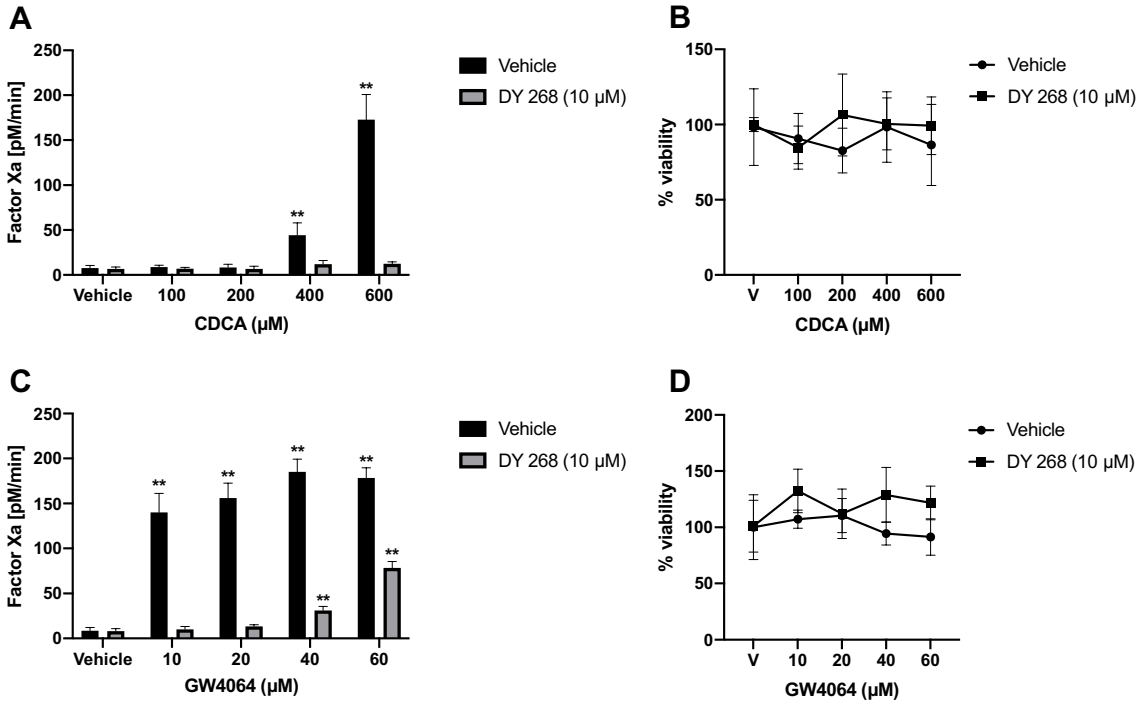

Figure 12. Addition of DY 268 reduces TF activity (112).

The impact of CDCA (100-600 µM) and GW4064 (10-60 µM) on TF activity was evaluated with and without addition of the FXR antagonist DY264 by determining the production of coagulation factor Xa (FXa) from HepG2 cells after 24 hours of exposure **(A/C)**. Additionally, the viability of cells was tested using an MTT assay **(B/D)**. **p<0.001 for difference from vehicle.

We conducted follow-up experiments using primary human hepatocytes. We observed a slight increase in TF activity after 24 hours of exposure to 100 µM and 200 µM CDCA (100 µM: 2.3±0.4 pM FXa/min; 200 µM: 2.7±1.1 pM FXa/min; vehicle: 1.1±0.7 pM FXa/min; p<0.05). Furthermore, a significant increase in TF activity was observed when exposed to 400 µM CDCA (5.2±0.5 pM FXa/min; p<0.001). Notably, contrary to HepG2 cells, TF activity was increased after exposure to GCDCA at all concentrations for 24h and was even higher than with CDCA (100 µM: 12.9±8.9 pM FXa/min; 200 µM: 13.1±6.4 pM FXa/min; 400 µM: 14.4±8.5 pM FXa/min; vehicle: 3.1±1.5 pM FXa/min; p<0.001; Fig. 13A).

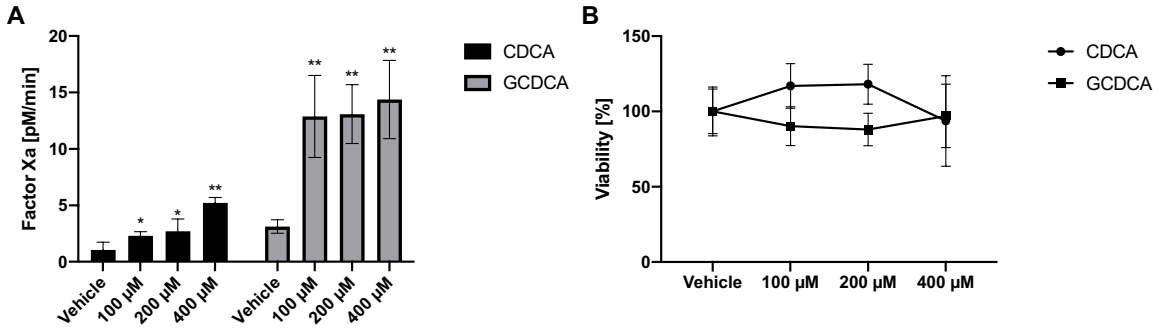

Figure 13. Increased TF activity in primary human hepatocytes after exposure to bile acids (112).

Primary human hepatocytes were incubated with 100, 200, or 400 µM of CDCA or GCDCA for 24 hours, with dimethyl sulfoxide utilized as the vehicle. Coagulation factor Xa (FXa) production was measured to analyze the tissue factor activity **(A)**. The cell viability was also evaluated using the MTT assay **(B)**. Data are presented as % viability of the cells and expressed as mean ± SD (N=6). * p<0.05 for difference from vehicle; ** p<0.001 for difference from vehicle.

In additional experiments, we exposed HepG2 cells to an endoplasmatic reticulum stressor tunicamycin for 24 hours and could observe a dose-dependent increase of TF activity at concentrations above 40 µM. Again, MTT tests showed intact cell viability at all concentrations of tunicamycin. (Fig. 14)

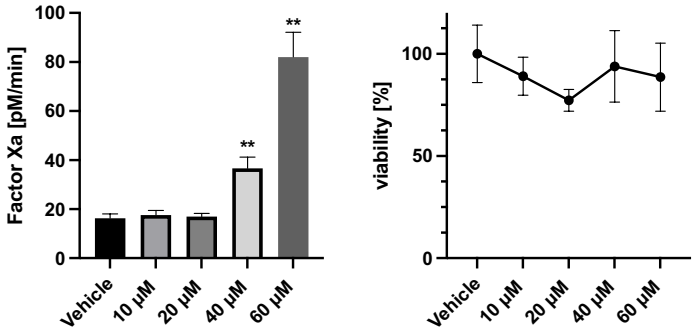

Figure 14. Increase of tissue factor (TF) activity in HepG2 cells after exposure to the ER-stressor tunicamycin for 24 hours.

TF activity was assessed via generation of coagulation factor Xa. Data are expressed as mean ± SD (N=6). MTT data are presented as % viability of the cells and expressed as mean ± SD (N=6). *p<0.05 for difference from vehicle; ** p<0.001 for difference from vehicle.

3.1.2 Thrombin generation assay

The effects of BA and GW4064 on thrombin generation curves are displayed in Table 2.

	Lag time [min]	Peak height [nM]	ETP [nM*min]
CDCA			
Vehicle	11.00±1.05	30.72±4.03	432.1±89.5
100µM	7.16±1.07**	35.83±5.69	556.0±76.1*
200µM	5.17±0.91**	36.31±5.61*	530.9±69.3*
400µM	3.78±1.14**	43.84±7,92**	640.6±91.4**
600µM	3.10±0,82**	44.55±5.41**	631.4±82.4**
GCDCA			
Vehicle	11.04±1.09	34.51±4.19	548.8±71.3
100µM	11.51±1.53	38.18±6.93	539.1±81.5
200µM	11.92±1.22	35.02±5.05	571.9±85.4
400µM	11.68±1.23	34.13±4.72	587.3±69.2
600µM	8.86±1.01	33.27±5.28	535.8±93.6
UDCA			
Vehicle	8.76±0,74	55.44±7.10	545.9±82.4
100µM	10.26±1.32*	47.08±6.89*	503.4±72.4
200µM	8.97±0.70	56.62±7.32	581.7±83.0
400µM	9.36±1.06	57.73±5.95	577.3±65.8
600µM	7.83±1.13	57.08±6.13	586.9±92.3
GW4064			
Vehicle	10.55±1.13	37.97±5.33	503.7±70.1
10µM	5.91±0.94**	46.61±5.59*	589.4±76.7*
20µM	3.56±0.98**	55.47±6.01**	611.7±79.4**
40µM	2.45±0.59**	69.60±7.13**	637.3±80.2**
60µM	2.54±0.69**	67.32±7.84**	629.5±76.7**

Table 2. Parameters of clotting cascade reactions after exposure of HepG2 cells to various bile acids or GW4064 (N=6) (112). *p<0.05; **p<0.001.

Of all the quantitative values deducible from the thrombin trace, the period of delay until the commencement of thrombin production (lagtime) was mainly affected by a pre-incubation of HepG2 cells with BA. A dose-dependent diminishing of the lagtime accompanied by a corresponding increase in ETP and Peak thrombin generation was evidently seen with CDCA and GW4064 (Figure 15A/D, Table 2; $p<0.001$) but not with UDCA and GCDCA (Figure 15B/C, Table 2, $p<0.001$). Interestingly, UDCA at the lowest dosage (100 µM) seemingly extended the lagtime to a slight degree compared to the control (Figure 15C).

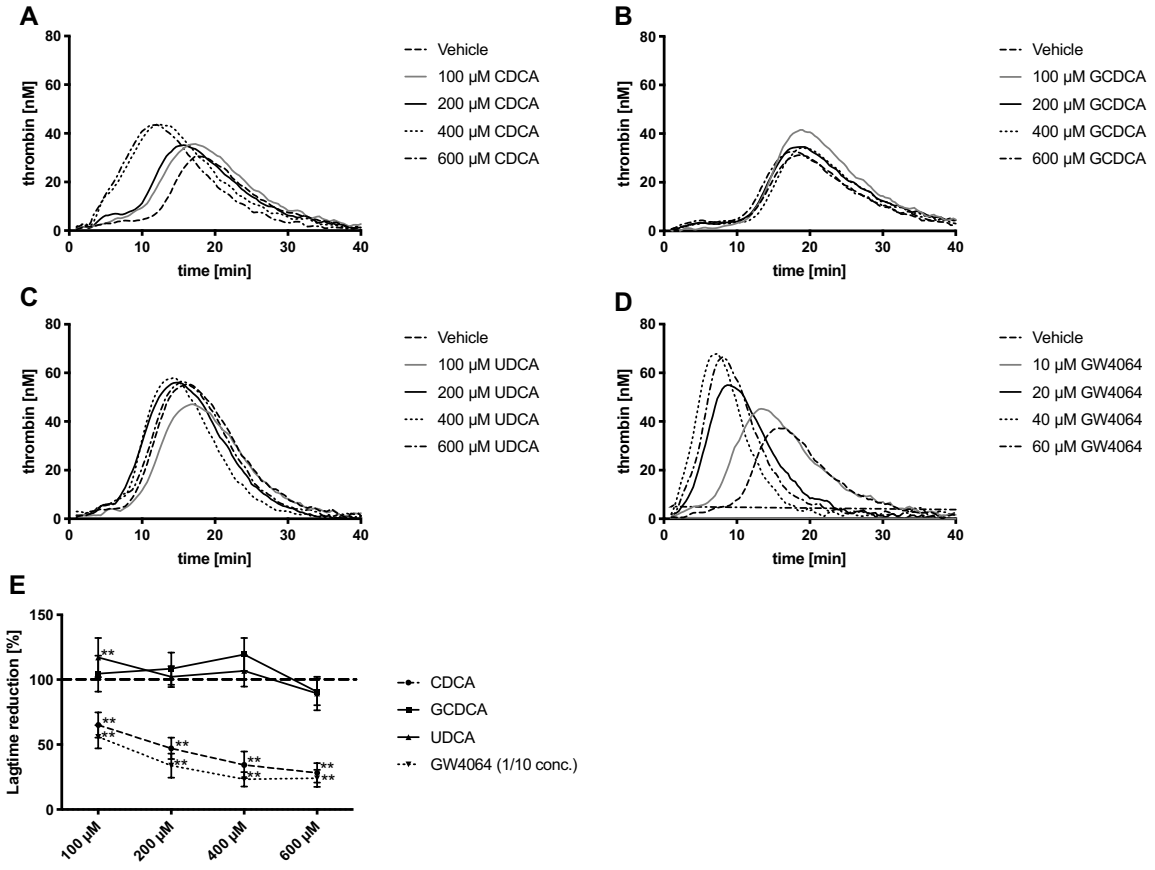

Figure 15. Representative thrombin generation curves and lagtime reduction after exposure of HepG2 cells with various bile acids (112).

The capacity of a sample to form thrombin was investigated with respect to the time before the thrombin outburst (lagtime) and the absolute amount of thrombin activity (endogenous thrombin potential), which was measured as the area beneath the curve. HepG2 cells were treated with 100, 200, 400, or 600 µM of **(A)** CDCA, **(B)** GCDCA, **(C)** UDCA, or **(D)** 1, 5, 10, or 40 µM of GW4064. Dimethyl sulfoxide acted as the control. Measurements were done after the addition of corn trypsin inhibitor to stop contact activation of clotting. **(E)** Percentage reduction/prolongation of lagtime triggered by different bile acids in various concentrations. Data are shown as mean ± SD (N=9). ** $p<0.01$ for comparison with control.

3.2 FXR activation

Alterations in the mRNA levels of FXR activation markers, as well as of TF, after incubation with 200 µM BA or 20 µM GW4064 are presented in Figure 16. The FXR targets OST-α and OST-ß were markedly increased in comparison to the DMSO control when cells were preincubated with CDCA or GW4064, whereas no effect was observed with GCDCA or UDCA.

The FXR target SHP showed a minor increase in expression compared to the DMSO control with CDCA or GW4064 after 12 hours but not after 24 hours of incubation. No effect was observed with GCDCA and UDCA. None of the utilized BA or GW4064 triggered upregulation of TF in any of the tested concentrations at any time point.

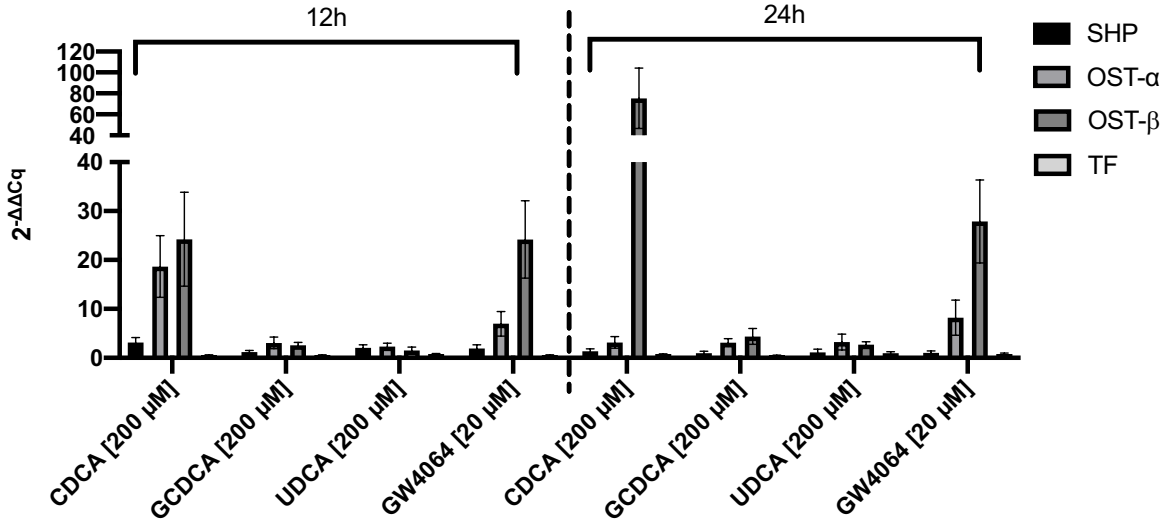

Figure 16. Expression of FXR targets after incubation with different BA or GW4064 (112).
Human HepG2 cells were incubated with a concentration of 200µM of CDCA, GCDCA, or UDCA, or 20µM of GW4064 for either 12 hours or 24 hours. Primers for SHP, OST-α, OST-ß, and tissue factor (TF) were used, with SHP, OST-α, and OST-ß being known FXR targets. To normalize the data, β-actin was employed, and relative gene expression was examined using the ΔΔCq method. ΔΔCq-values were standardized to dimethyl sulfoxide. The results are presented as average fold change (2-ΔΔCq) (N=2).

Table 3 shows 2–ΔΔCq values of all tested concentrations.

	SHP	OST-α	OST-ß	TF
12 hours				
100μM CDCA	2.20	5.88	10.25	0.28
200μM CDCA	3.16	18.67	24.27	0.38
400μM CDCA	1.72	2.25	6.77	2.13
100μM GCDCA	1.26	2.04	1.78	0.21
200μM GCDCA	1.19	3.06	2.56	0.38
400μM GCDCA	1.71	4.46	3.19	0.72
100μM UCDCA	1.39	2.06	1.69	0.51
200μM UCDCA	2.04	2.27	1.49	0.59
400μM UCDCA	1.15	2.51	2.36	1.15
1μM GW4064	1.65	4.24	10.19	0.34
5μM GW4064	1.96	7.03	12.20	0.26
10μM GW4064	2.23	7.52	22.95	0.35
20μM GW4064	1.94	6.98	24.19	0.37
40μM GW4064	1.17	6.84	22.49	0.25
24 hours				
100μM CDCA	0.58	6.75	7.96	0.41
200μM CDCA	1.34	3.16	75.20	0.57
400μM CDCA	0.49	0.97	6.79	0.99
100μM GCDCA	0.99	1.90	2.08	0.46
200μM GCDCA	0.92	3.11	4.37	0.34
400μM GCDCA	2.13	4.04	7.13	0.45
100μM UCDCA	1.02	1.98	2.65	0.65
200μM UCDCA	1.15	3.23	2.70	0.82
400μM UCDCA	0.91	1.66	2.64	0.95
1μM GW4064	1.33	7.42	24.08	0.67
5μM GW4064	1.26	8.68	28.15	0.57
10μM GW4064	1.05	5.45	23.08	0.56
20μM GW4064	1.32	9.06	29.50	0.62
40μM GW4064	1.02	8.21	27.87	0.62

Table 3. $2^{-\Delta\Delta Cq}$ values of FXR targets (SHP, OST-α, OST-ß) and tissue factor (TF) after incubation of HepG2 cells with CDCA, GCDCA, UCDCA, or GW4064 in various concentrations (N=2) (112).

3.3 TF protein expression

Western blot experiments indicated no augmentation of TF protein quantities following the exposure of HepG2 cells to CDCA, GCDCA, UDCA, or GW4064 for 24 hours in all concentrations employed for TF activity assessment (Fig. 17A-D). Quantification of blot bands normalized to GAPDH revealed no meaningful variation in TF protein expression levels (Fig. 17E).

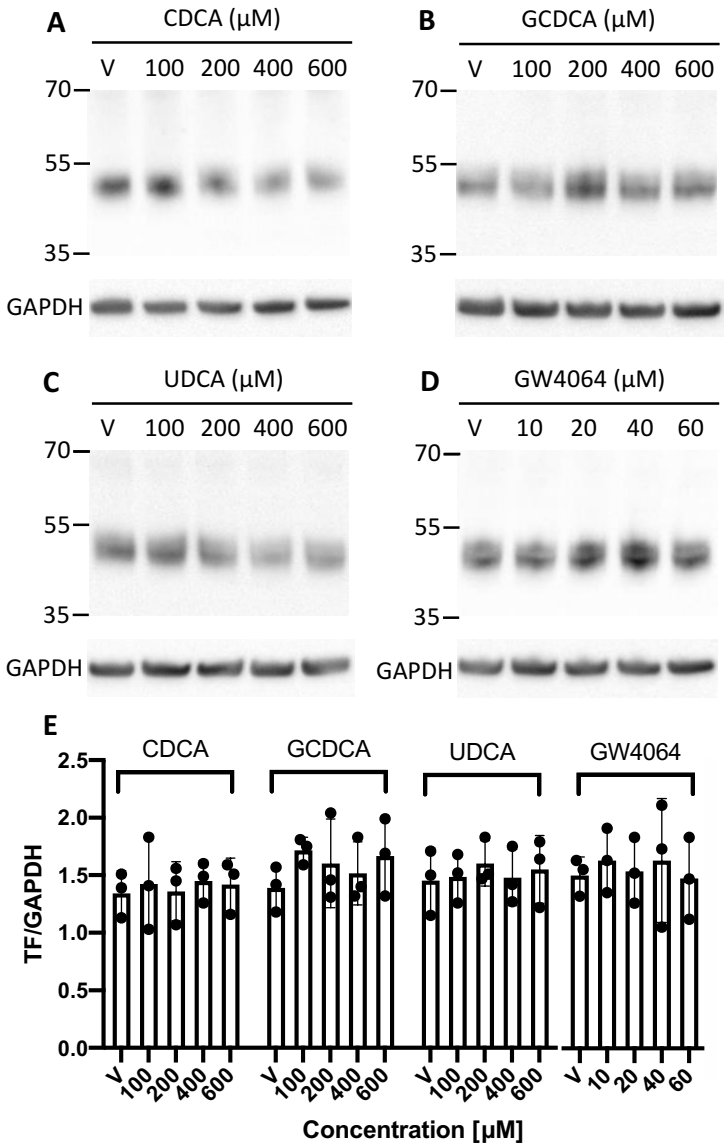

Figure 17. Protein expression of TF after exposure to BA or GW4064 (112).
(A-D) Representative Western blot results of TF following exposure of HepG2 cells to CDCA, GCDCA, UDCA (100-600 µM), or GW4064 (10-60 µM). Dimethyl sulfoxide served as the vehicle and GAPDH was utilized as the control. **(E)** Densitometric analysis with normalization to GAPDH from three independent experimental replicates.

Fluorescence microscopy images of stained HepG2 cells did not display an increase or rearrangement of TF after 24 hours exposure to CDCA, GCDCA, UDCA (600 µM), or GW4064 (60 µM).(Figure 18).

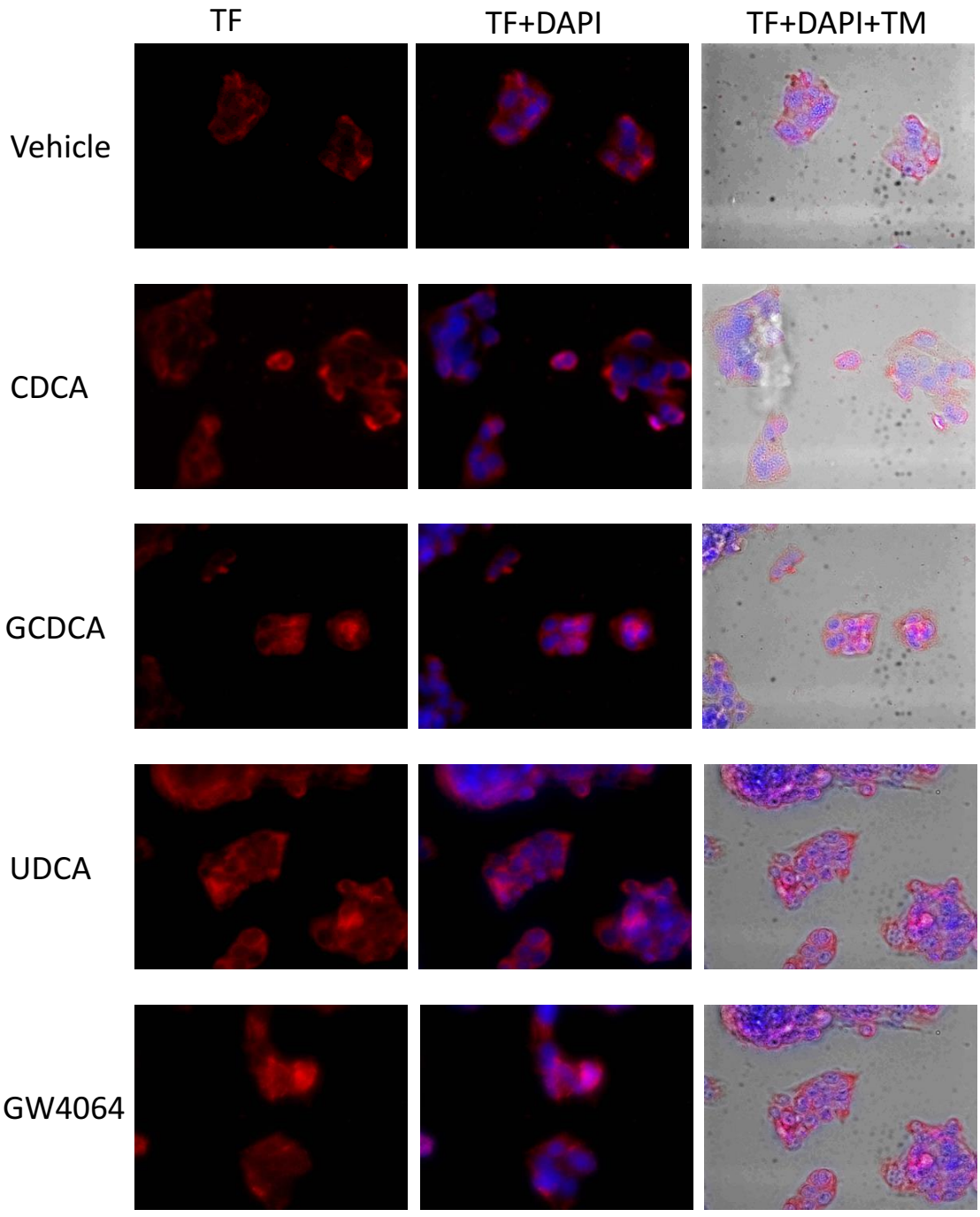

Figure 18. Fluorescence images of HepG2 cells stained for TF (112).

HepG2 cells were incubated with 600μM CDCA, GCDCA, UDCA, or GW4064 for 24h. Cells were fixed and stained with an Alexa Fluor 488 conjugated TF antibody and DAPI. No significant upregulation or redistribution of TF was observed (N=3).

3.4 Cell viability and apoptosis

3.4.1 MTT assay

The results of the MTT tests showed that the viability of HepG2 cells and primary hepatocytes remained unaltered during all experiments (Fig. 11C/Fig. 13B). Neither GCDCA nor UCDCA had a negative effect on HepG2 cell viability when concentrations were up to 1500 µM. However, CDCA had a notable decrease in cell viability when concentrations exceeded 1000 µM (Fig. 11C). For GW4064, the cell viability remained consistent up to 60 µM, however, decreased when the concentration was 100 µM (Fig. 11D).

3.4.2 LDH cytotoxicity assay

The LDH-Cytotoxicity Assay displayed no discernible leakage of LDH from HepG2 cells following 24 hours with BA amounts up to 600 µM (Fig. 11E). A slight rise in LDH release was detected at quite elevated GW4064 amounts (100 µM) (Fig. 11F).

3.4.3 Caspase-3 activity

Following a 24 hour exposure to CDCA, GCDCA, UDCA (100–600 µM), or GW4064 (1–60 µM) there was no observable rise in caspase-3 activity. Conversely, incubation with staurosporine (2–4µM) as a positive control generated a considerable boost in caspase-3 activity (Fig. 19).

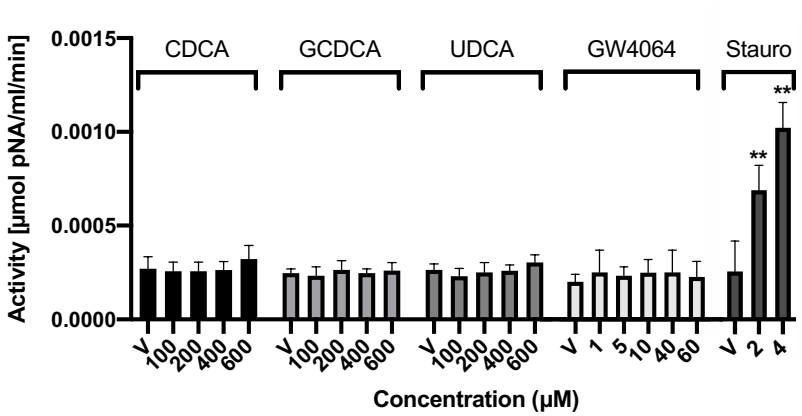

Figure 19. Caspase-3 activity in HepG2 cells after exposure to BA, GW4064, or staurosporine (112).

HepG2 cells were exposed to CDCA, GCDCA, and UDCA (100-600µM), GW4064 (1-60 µM), or staurosporine (2-4 µM) for a period of 24 hours. Dimethyl sulfoxide was employed as the control. Caspase-3 activity was measured using a colorimetric assay based on the liberation of p-nitroaniline (pNA) from a peptide substrate (Ac-DEVD-pNA). Data are represented as mean ± SD (N=6). ** Statistically significant difference from the control at the $p<0.01$ level.

3.4.4 Flow cytometry

Even at substantially elevated BA concentrations (600 µM), no detectable change in the fluorescence readings of propidium iodide or Annexin V indicative of necrotic or apoptotic processes was observed in any population (Figure 20).

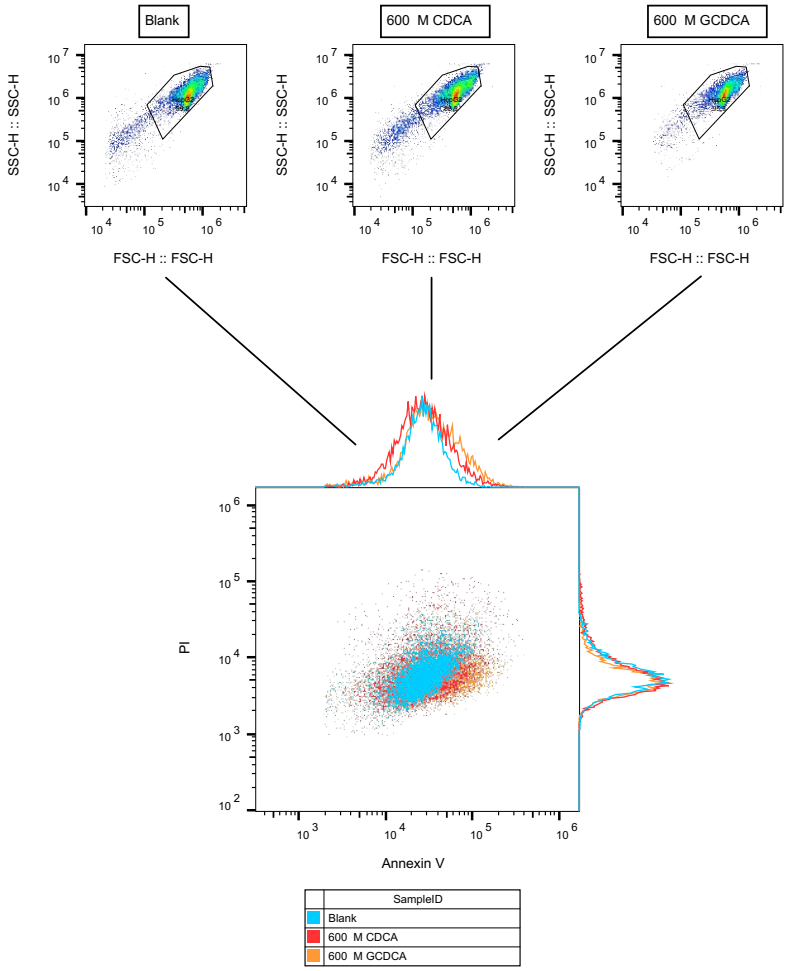

Figure 20. Flow cytometry (112).

HepG2 cells were incubated with 600µM of chenodeoxycholic acid (CDCA) or glycochenodeoxycholic acid (GCDCA) for 24h and stained with fluorescein isothiocyanate conjugated Annexin V and propidium iodide (PI). No significant shift in Annexin V binding was observable in any population (N=6).

4 Discussion

There are contradictory opinions concerning the implications of BA-induced coagulation on the progression of cholestatic liver disease. We learned from fibrin deposits in mouse models that blood coagulation and cholestasis interact in some kind of way. Until today, the exact mechanism and/or triggers of coagulation in a cholestatic setting is unclear (102-106).

In this study, the effect of BA on TF-activity and thrombin generation in hepatocytes was investigated.

4.1 The potential of different BA to induce TF activity

After incubation of HepG2 cells with CDCA increased TF activity could be denoted. No effects were observed with GCDCA and UDCA. Alongside, enhanced thrombin generation, marked by shortened lag time and increased ETP in CAT analysis could be demonstrated with CDCA. Again, GCDCA and UDCA did not influence thrombin generation in HepG2 cells.

Control experiments with primary human hepatocytes were performed: Interestingly, enhanced TF activity could also be observed with GCDCA. A possible explanation is the fact that in contrast to unconjugated BA, conjugated BA need active transportation into the liver cell, which is usually facilitated by the sodium taurocholate cotransporting polypeptide (NTCP) (113), which HepG2 cells do not express (114). Consequently, GCDCA was not able to enter HepG2 cells, denoted by the absence of an effect in the TF activity assay.

It should be mentioned that the effects on TF activation and thrombin generation in HepG2 cells were observed at unphysiologically high BA concentrations; however, with primary hepatocytes the same effects could be denoted at lower concentrations, possibly occurring in a cholestatic setting.

4.2 The role of FXR in TF activation

As mentioned above, we observed increased TF activity in HepG2 cells with CDCA but not with GCDCA, arguing for a mechanism, where BA have to enter hepatocytes to induce TF

activity. To test this hypothesis, HepG2 cells were incubatied with various BA and quantitative PCR of FXR targets SHP, OST-α and OST-ß was performed, since FXR is a nuclear BA receptor and pivotal for liver metabolism (115). Alongside with their ability to induce TF activity, upregulation of SHP, OST-α and OST-ß was observed with CDCA and but not with GCDCA and UDCA.

To elucidate whether the potential of BA to induce TF is linked specifically to FXR activation, we employed GW4064, a potent synthetic FXR agonist that is structurally different from BA. Enhanced TF activity and thrombin generation after incubation with GW4064 was demonstrated in HepG2 cells, as well as in primary hepatocytes. GW4064 does not have the steroid structure of BA, therefore it can be deduced that TF decryption in context with various BA does not only depend on their physicochemical properties but on intracellular signaling involving the nuclear receptor FXR.

As a control experiment, FXR was blocked with the synthetic antagonist DY268. In the presence of DY268 no effects on TF activity with CDC and reduced effects with GW4064 were observed.

Thus, it can be hypothesized that indeed TF decryption via BA is more likely a process involving intracellular FXR-dependent signaling than a phenomenon purely based on changes on the cell membrane. Thus, FXR activation could be essential for triggering local coagulatory effects.

4.3 The nature of TF activation

To investigate whether TF expression is influenced by FXR activation, we performed qPCR of F3 encoding TF and found no upregulation. Alternatively, there could be a shift from intracellular TF to the plasma membrane, leading to procoagulant changes of the membrane. However, in florescence microscopy no significant upregulation or redistribution of TF was observed.

Thus, the effects are likely due to enhancement of already expressed TF activity via conformational changes. Consequently, there seems to be an unknown intermediate step after FXR activation via BA that ultimately leads to TF decryption.

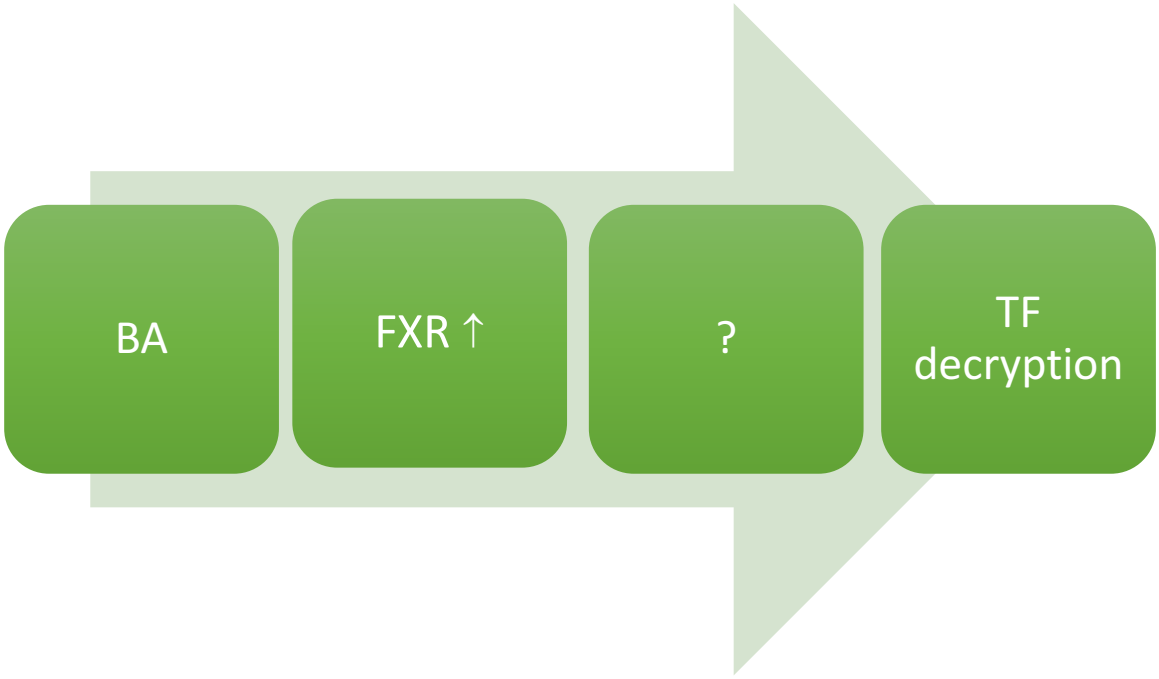

Figure 21. Illustration of mechanism of TF decryption via BA.

4.4 Possible other signaling contributors

4.4.1 Apoptosis

A number of experiments were performed to prove that the observed effects were not connected to possible cell death mechanisms: Firstly, all used BA concentrations were below the critical micellar concentration (116), thereby excluding cell damage by saponification. MTT tests assays were performed throughout all experiments, ensuring the viability of all cells, HepG2 cells as well as primary hepatocytes, during the performed experiments. Also, the cytotoxicity assay showed no LDH release at the employed BA concentrations.

Alterations of the phospholipid composition of the cell membrane ("Flip-flop effect") was a previously mentioned theory of TF decryption (14), and loss of lipid asymmetry is a feature associated with apoptosis (117). Therefore, caspase-3 cleavage and phosphatidylserine expression as markers of apoptosis were evaluated. Neither caspase-3 cleavage, nor an increase in phosphatidylserine expression detectable by Annexin V binding in flow cytometry was observable. These findings are supported by the fact that HepG2 is a

hepatoblastoma-derived cell line, inherently refractory to apoptosis. It can thus be concluded that enhanced TF activity and thrombin generation were not due to apoptotic changes of the plasma cell membrane.

4.4.2 Acid sphingomyelinase

A novel mechanism of TF regulation has been proposed by Wang et al.: They discovered that sphingomyelin, a protein located in the outer leaflet of the plasma cell membrane of e.g. macrophages is responsible for keeping TF in an encrypted state (92). Acid sphingomyelinase (ASM) induces TF decryption, promoting procoagulant activity (91).
Sars Cov-2 virus, the cause of a global pandemic, has been constantly discussed in and outside medical literature in the past months. Wang et al. showed that infection with the Sars Cov-2 spike protein virus leads to activation of ASM, followed by enhanced TF activity, thereby explaining at least in part the observed hypercoagulable state in COVID-19 patients (118).

Endoplasmatic reticulum (ER) stress seems to be a key player in activation of ASM and has been observed as trigger for ASM-induced apoptosis in macrophages (119). However, ASM-dependent actions seem not to be FXR-linked and a role of ASM in hepatocytes has not been shown yet.

4.4.3 Protein disulfide isomerase / endoplasmatic reticulum stress

As mentioned above, the exact mechanism of TF decryption via FXR overstimulation in a cholestatic setting is unclear. Our study group postulates that long-term rather than short-term BA exposure of cells leads to initiation of coagulation processes. We propose a mechanism in which signaling overload leads to endoplasmatic reticulum (ER) stress. ER stress is known to be followed by an unfolded protein response (UPR), ultimately leading to the secretion of chaperones in liver cells. Principally UPR is a physiological mechanism and crucial to maintain homeostasis in liver metabolism via protection against ER stress. However, if ER stress cannot be adequately relieved, UPR leads to cell death, promoting hepatocyte apoptosis and fibrosis via activation of hepatic stellate cells (120, 121). This mechanism seems to facilitate the progression of various liver diseases (122). Previous studies have shown that BA can induce unfolded protein response, at least upon direct interaction with proteins (123). FXR activation, however, has been shown to inhibit ER stress in hepatocytes and thereby limiting hepatic inflammation and ameliorating liver injury

(124). However, hepatic FXR stimulation and upregulation of SHP seems to directly activate UPR involving inositol-requiring enzyme 1α (IRE1α) and X-box binding protein 1 (XBP1) (125). One of the chaperones upregulated by the IRE1α/XBP1 mediated UPR is protein disulfide isomerase (PDI) (126). Increased PDI expression in rat hepatocytes after incubation with ER stressor tunicamycin was observed, thus confirming the association between increased PDI release and UPR (127). PDI release was also linked to TF decryption on monocytes and keratinocytes and to contribute to procoagulant mechanisms in vivo (90, 128-130).

Our study group performed experiments with HepG2 cells where we could observe increased TF activity after incubation with tunicamycin in a dose-dependent manner. These findigs hint to TF decryption by UFP.

Hence, we hypothesize that long-term exposure of hepatocytes to pathologically high BA concentrations triggers UPR via FXR overstimulation, and the resulting surge in PDI expression leads to increased TF activity triggering thrombin generation which ultimately promotes liver injury and fibrosis. Our hypothesis is illustrated in Figure 22. Studies to test this hypothesis will be conducted.

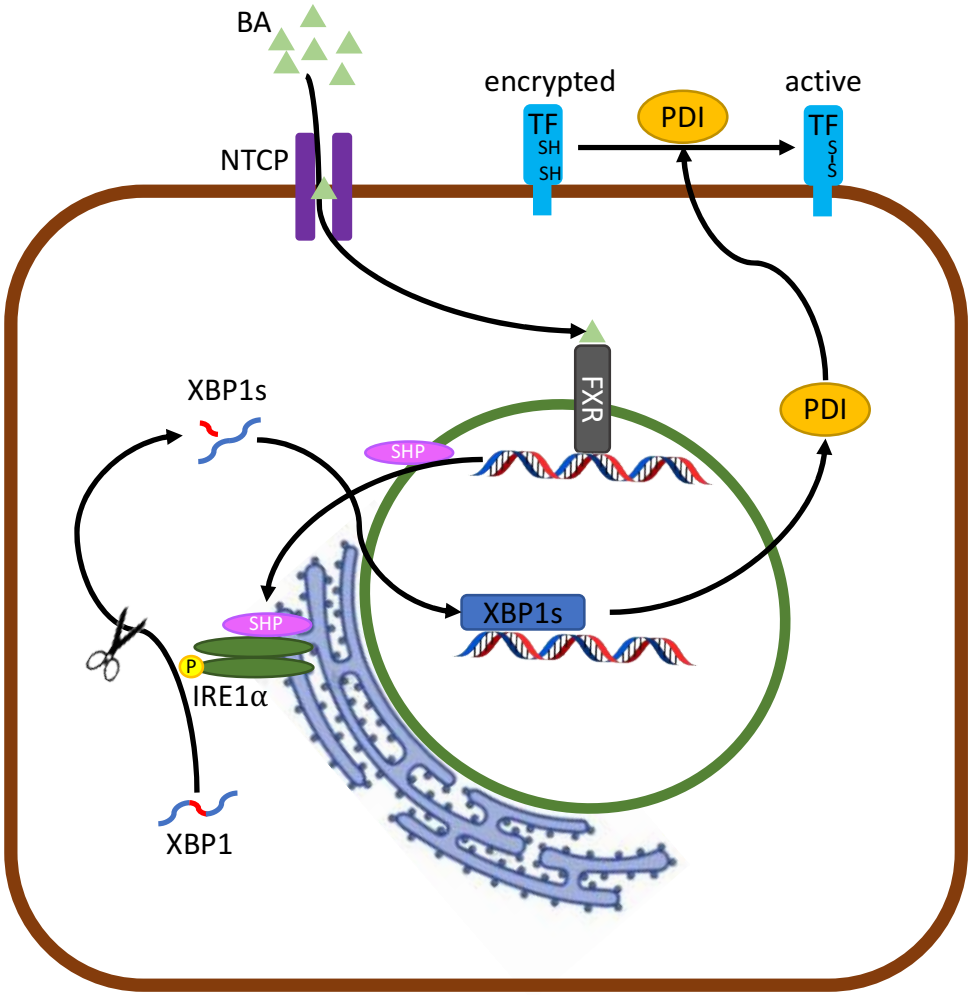

Figure 22. Proposed mechanism of TF decryption

BA enter the hepatocyte through NTCP, stimulate the nuclear receptor FXR, leading to upregulation of SHP, inducing ER stress. As a result, XBP1 and IRE1α-mediated UFP leads to shedding of PDI and decryption of TF.

4.5 Differences from previous findings

Our findings complement a recent study by Baker et al. who demonstrated that BA directly accelerate TF/FVIIa complex activation, even in the absence of phospholipids (108). Compared to the present study, partially divergent results were obtained by Baker et al.: First of all, by using primary human hepatocytes for all their experiments, they could demonstrate effects with GCDCA, which we could not observe in our experiments with HepG2 cells. The above-mentioned explanation is simply the lack of NTCP of HepG2 cells, thereby preventing intracellular uptake of GCDCA, denoted by the absence of FXR activation in qPCR. However, as explained above, this indicates further that the observed procoagulant activities of BA are based on intracellular mechanisms, rather than on cell

membrane changes.

Secondly, in contrast to our findings, Baker et al. did not observe effects with FXR agonist GW4064. It can only be speculated that this might be due to the varying incubation times: While Baker et al. incubated their cells for 30 minutes, we performed our experiments after incubation for 12 hours and 24 hours respectively and observed that TF procoagulant activity not only increased with time but took several hours to be detectable. Clinically, this might hint to procoagulant changes in liver cells due to long-term exposure to high BA concentrations in a setting of chronic cholestasis. Prolonged FXR stimulation could cause alterations in intracellular signalling that could bring about the decryption of TF. The lack of an immediate reaction is presumably a protective mechanism because rapid bile acid-induced TF activation could impair the FXR mediated regulation of bile acid production in the liver.

Lastly, Baker et al. postulated direct effects of BA on TF/VIIa complex activation. In the present study accelerated TF activity and subsequent thrombin generation was observed even after *removal* of BA from the cells. In CAT analyses, increased ETP and reduced lag time was observed with preincubated HepG2 cells without addition of external TF. Thus, it can be postulated that BA are not only co-factors for TF activation but act as ligands causing intracellular signaling, thereby facilitating TF decryption.

4.6 Potential translational implications

UDCA is a frequently used drug in children and adults suffering from all kinds of cholestatic liver diseases or diseases accompanied by liver impairement, like cystic fibrosis and drug induced liver injury. (16, 29, 55-58). It has been shown to slow down disease progression and to improve serum liver parameters, at least temporarily (3). Besides, it has a favourable safety profile if administered in medium doses (29, 131). High doses of UDCA have been reported to be harmful in terms of adverse events in patients suffering from primary sclerosing cholangitis (60). Common adverse effects of UDCA include diarrhea, abdominal pain and skin reactions, as well as metabolic drug interactions (59). So far, alterations in the blood coagulation system have not been reported in connection with UDCA. Physicochemically, UDCA is less hydrophobic compared to other BA as CDCA and GCDCA and UDCA is seen (at least in part) as FXR antagonist (132). In the present study, it could be demonstrated that UDCA does not accelerate TF activity or induce increased thrombin generation in an in-vitro setting. On the contrary: After incubation of HepG2 cells with 100

μM UDCA, the lagtime was reproducibly prolongued, indicating a slight protective effect at this dose in regard to procoagulant features. Thus, UDCA has no relevant effect on coagulation activation in vitro and seems to be a safe therapeutic agent in terms of coagulation aspects. Basic as well as translational experiments on the effects of novel therapeutic BA for adult cholestatic liver diseases, such as norUDCA and OCA, on TF activity and throbin generation might be desirable.

It was demonstrated that chronic inflammatory conditions such as in IBD exhibit the potential to locally activate coagulation processes, not only by platelet activation but also by alterations of the mucosal barrier (133-135). Since long-term exposure to high BA levels in chronic cholestasis is believed to be accompanied or at least mediated by local inflammatory processes in the liver (136), it can be speculated that local coagulation activation similar to inflammatory bowel disease might be present. Moreover, in prior investigations, fibrin deposits were found in portal fields in animal models of cholestatic liver injury (102, 103). This too hints to activation of local coagulation phenomena via elevated BA concentrations. Through the present investigations, it was confirmed that some BA can trigger local coagulation activation, depending on their concentration and hydrophobicity. However, the exact pathophysiological mechanisms leading to intrahepatic fibrin deposits are also dependent on the unique microenvironment inside the liver and the space of Disse, which was not entirely simulated in the present in vitro experiments.

C-6-alpha and 6-beta hydroxylated BA, so-called aBA, have been identified in neonates in health and disease as well as in adults with cholestatic liver disease (41, 42, 137). Recently, the role of aBA in itch has been evaluated (138). In the present study, no aBA have been investigated. Considering the observed link between “typical” BA with coagulation processes, further exploration of the role aBA in TF activation and thrombin generation might be warranted to elucidate potential procoagulant features triggered by aBA in neonates.

Taken together, the present findings suggest that long-term exposure of hepatocytes to nontoxic BA can lead to TF activation and TF-induced thrombin generation via FXR-pathway independently of apoptotic mechanisms. This could be a new pathway in the progression of cholestatic liver diseases in children and adults. Further studies will assess the longitudinal impact of specific BA compositions on the coagulation activation potential in cholestatic patients. Results from this and future studies may have major implications for the design of therapeutic agents targeting cooperative players involved in aforementioned signaling.

4.7 Strengths and limitations

To our knowledge, this is the first report of BA triggering coagulation activation via intracellular signaling involving the nuclear BA receptor FXR. A variety of experiments were performed to confirm the hypothesis and to rule out potential confounding factors (e.g. cell death as cause for TF activation).

The drawbacks of these in vitro experiments involve the utilization of an isolated chemical milieu for the cells and serum for the CAT measurements. Even though the Disse space offers physiological interaction between hepatocytes and plasma proteins, it was not feasible to precisely imitate the natural environment of hepatic tissue.

Furthermore, the author acknowledges that the in vitro simulation of coagulation activation in liver cells is no adequate replacement for in vivo studies. When using animal models of cholestasis, bile duct ligation seems to resemble a model of acute more than chronic cholestasis. FXR-knockout mice would be more suitable to mimic chronic cholestasis. However, it is not feasible to carry out research that delves into the details of TF decryption in a living organism, as obtaining samples from liver biopsies or homogenizing livers taken from animal models can alter the environment that surrounds TF and change its conformation.

Also, cell death could falsify the results: To test local TF activation, livers of mice would have to be extracted, thereby inducing apopototic mechanisms in the cells. The same dilemma is true for experiments with human livers, e.g. when using liver biopsy samples. The harvesting procedure (core needle biopsy) will lead to cell death and alterations of coagulation processes.

4.8 Conclusion

There are conflicting statements in literature as to whether coagulation drives or limits the progression of liver disease in a cholestatic setting. The aim of this study was to answer key questions concerning the influence of BA on TF activation and thrombin generation, as well as the mechanism behind potential BA-induced TF activation.

In summary, it was demonstrated that BA are able to induce TF activity and thrombin generation in hepatocytes, depending on their concentration and hydrophobicity. TF activation occurred independently of the amphiphilic properties of BA and in the absence of apoptosis.These effects occur by TF decryption via intracellular FXR overstimulation rather than transcriptional upregulation of TF expression.

Prolonged contact of hepatocytes with increased levels of endogenous BA like CDCA can lead to decryption of TF and an increase in thrombin generation induced by TF. These effects are associated with the activation of the FXR pathways and appear to be unrelated to apoptotic processes. UDCA seems to be a secure medication with regards to its effects on intrahepatic coagulation.

To our knowledge this is the first report of BA-induced TF decryption via intracellular FXR signaling.

Further studies will be necessary to assess the in-vivo relevancy of our findings. The longitudinal impact of specific BA compositions on the coagulation activation potential in cholestatic patients should be elucidated. Results from this and future studies may have shed light into the link between coagulation and cholestasis and have implications on future therapies of cholestatic liver diseases.

5 References

1. Hofmann AF. Bile Acids: The Good, the Bad, and the Ugly. News Physiol Sci. 1999;14:24-9.
2. Hofmann AF, Hagey LR. Bile acids: chemistry, pathochemistry, biology, pathobiology, and therapeutics. Cell Mol Life Sci. 2008;65(16):2461-83.
3. Trauner M, Graziadei IW. Review article: mechanisms of action and therapeutic applications of ursodeoxycholic acid in chronic liver diseases. Alimentary pharmacology & therapeutics. 1999;13(8):979-96.
4. Hofmann AF. The continuing importance of bile acids in liver and intestinal disease. Arch Intern Med. 1999;159(22):2647-58.
5. Trauner M, Claudel T, Fickert P, Moustafa T, Wagner M. Bile acids as regulators of hepatic lipid and glucose metabolism. Digestive diseases (Basel, Switzerland). 2010;28(1):220-4.
6. Lefebvre P, Cariou B, Lien F, Kuipers F, Staels B. Role of bile acids and bile acid receptors in metabolic regulation. Physiol Rev. 2009;89(1):147-91.
7. Saeed A, Hoekstra M, Hoeke MO, Heegsma J, Faber KN. The interrelationship between bile acid and vitamin A homeostasis. Biochim Biophys Acta Mol Cell Biol Lipids. 2017;1862(5):496-512.
8. Theiler-Schwetz V, Zaufel A, Schlager H, Obermayer-Pietsch B, Fickert P, Zollner G. Bile acids and glucocorticoid metabolism in health and disease. Biochim Biophys Acta Mol Basis Dis. 2019;1865(1):243-51.
9. Chiang JY. Bile acid metabolism and signaling. Compr Physiol. 2013;3(3):1191-212.
10. Russell DW. The enzymes, regulation, and genetics of bile acid synthesis. Annu Rev Biochem. 2003;72:137-74.
11. Thomas C, Pellicciari R, Pruzanski M, Auwerx J, Schoonjans K. Targeting bile-acid signalling for metabolic diseases. Nat Rev Drug Discov. 2008;7(8):678-93.
12. Huang WM, Gowda M, Donnelly JG. Bile acid ratio in diagnosis of intrahepatic cholestasis of pregnancy. Am J Perinatol. 2009;26(4):291-4.
13. Jericho HS, Kaurs E, Boverhof R, Knisely A, Shneider BL, Verkade HJ, et al. Bile acid pool dynamics in progressive familial intrahepatic cholestasis with partial external bile diversion. J Pediatr Gastroenterol Nutr. 2015;60(3):368-74.
14. Suga T, Yamaguchi H, Sato T, Maekawa M, Goto J, Mano N. Preference of Conjugated Bile Acids over Unconjugated Bile Acids as Substrates for OATP1B1 and OATP1B3. PloS one. 2017;12(1):e0169719.
15. Zohrer E, Resch B, Scharnagl H, Schlagenhauf A, Fauler G, Stojakovic T, et al. Serum bile acids in term and preterm neonates: A case-control study determining reference values and the influence of early-onset sepsis. Medicine (Baltimore). 2016;95(44):e5219.
16. Lazaridis KN, Gores GJ, Lindor KD. Ursodeoxycholic acid 'mechanisms of action and clinical use in hepatobiliary disorders'. Journal of hepatology. 2001;35(1):134-46.
17. Trauner M, Boyer JL. Bile salt transporters: molecular characterization, function, and regulation. Physiol Rev. 2003;83(2):633-71.
18. Kullak-Ublick GA, Stieger B, Hagenbuch B, Meier PJ. Hepatic transport of bile salts. Semin Liver Dis. 2000;20(3):273-92.
19. Kullak-Ublick GA, Beuers U, Paumgartner G. Hepatobiliary transport. Journal of hepatology. 2000;32(1 Suppl):3-18.
20. Xia X, Francis H, Glaser S, Alpini G, LeSage G. Bile acid interactions with cholangiocytes. World journal of gastroenterology. 2006;12(22):3553-63.
21. Ballatori N, Li N, Fang F, Boyer JL, Christian WV, Hammond CL. OST alpha-OST beta: a key membrane transporter of bile acids and conjugated steroids. Front Biosci (Landmark Ed). 2009;14(8):2829-44.

22. Mekhjian HS, Phillips SF, Hofmann AF. Colonic absorption of unconjugated bile acids: perfusion studies in man. Digestive diseases and sciences. 1979;24(7):545-50.
23. Dawson PA, Hubbert M, Haywood J, Craddock AL, Zerangue N, Christian WV, et al. The heteromeric organic solute transporter alpha-beta, Ostalpha-Ostbeta, is an ileal basolateral bile acid transporter. The Journal of biological chemistry. 2005;280(8):6960-8.
24. Kramer W, Sauber K, Baringhaus KH, Kurz M, Stengelin S, Lange G, et al. Identification of the bile acid-binding site of the ileal lipid-binding protein by photoaffinity labeling, matrix-assisted laser desorption ionization-mass spectrometry, and NMR structure. The Journal of biological chemistry. 2001;276(10):7291-301.
25. Wilson FA, Burckhardt G, Murer H, Rumrich G, Ullrich KJ. Sodium-coupled taurocholate transport in the proximal convolution of the rat kidney in vivo and in vitro. The Journal of clinical investigation. 1981;67(4):1141-50.
26. Chiang JYL, Ferrell JM. Bile Acid Metabolism in Liver Pathobiology. Gene Expr. 2018;18(2):71-87.
27. Moraes LA, Unsworth AJ, Vaiyapuri S, Ali MS, Sasikumar P, Sage T, et al. Farnesoid X Receptor and Its Ligands Inhibit the Function of Platelets. Arterioscler Thromb Vasc Biol. 2016;36(12):2324-33.
28. Parks DJ, Blanchard SG, Bledsoe RK, Chandra G, Consler TG, Kliewer SA, et al. Bile acids: natural ligands for an orphan nuclear receptor. Science. 1999;284(5418):1365-8.
29. Beuers U, Trauner M, Jansen P, Poupon R. New paradigms in the treatment of hepatic cholestasis: from UDCA to FXR, PXR and beyond. Journal of hepatology. 2015;62(1 Suppl):S25-37.
30. Carotti A, Marinozzi M, Custodi C, Cerra B, Pellicciari R, Gioiello A, et al. Beyond bile acids: targeting Farnesoid X Receptor (FXR) with natural and synthetic ligands. Curr Top Med Chem. 2014;14(19):2129-42.
31. Halilbasic E, Claudel T, Trauner M. Bile acid transporters and regulatory nuclear receptors in the liver and beyond. Journal of hepatology. 2013;58(1):155-68.
32. Wang YD, Chen WD, Moore DD, Huang W. FXR: a metabolic regulator and cell protector. Cell Res. 2008;18(11):1087-95.
33. Grober J, Zaghini I, Fujii H, Jones SA, Kliewer SA, Willson TM, et al. Identification of a bile acid-responsive element in the human ileal bile acid-binding protein gene. Involvement of the farnesoid X receptor/9-cis-retinoic acid receptor heterodimer. The Journal of biological chemistry. 1999;274(42):29749-54.
34. Goodwin B, Jones SA, Price RR, Watson MA, McKee DD, Moore LB, et al. A regulatory cascade of the nuclear receptors FXR, SHP-1, and LRH-1 represses bile acid biosynthesis. Mol Cell. 2000;6(3):517-26.
35. Edwards PA, Kast HR, Anisfeld AM. BAREing it all: the adoption of LXR and FXR and their roles in lipid homeostasis. J Lipid Res. 2002;43(1):2-12.
36. Stayrook KR, Bramlett KS, Savkur RS, Ficorilli J, Cook T, Christe ME, et al. Regulation of carbohydrate metabolism by the farnesoid X receptor. Endocrinology. 2005;146(3):984-91.
37. Wang X, Krupczak-Hollis K, Tan Y, Dennewitz MB, Adami GR, Costa RH. Increased hepatic Forkhead Box M1B (FoxM1B) levels in old-aged mice stimulated liver regeneration through diminished p27Kip1 protein levels and increased Cdc25B expression. The Journal of biological chemistry. 2002;277(46):44310-6.
38. Yang F, Huang X, Yi T, Yen Y, Moore DD, Huang W. Spontaneous development of liver tumors in the absence of the bile acid receptor farnesoid X receptor. Cancer Res. 2007;67(3):863-7.
39. Kim I, Morimura K, Shah Y, Yang Q, Ward JM, Gonzalez FJ. Spontaneous hepatocarcinogenesis in farnesoid X receptor-null mice. Carcinogenesis. 2007;28(5):940-6.

40. Shoda J, Mahara R, Osuga T, Tohma M, Ohnishi S, Miyazaki H, et al. Similarity of unusual bile acids in human umbilical cord blood and amniotic fluid from newborns and in sera and urine from adult patients with cholestatic liver diseases. Journal of Lipid Research. 1988;29(7):847-58.
41. Nakagawa M, Setchell K. Bile acid metabolism in early life: studies of amniotic fluid. Journal of lipid research. 1990;31(6):1089-98.
42. Zohrer E, Meinel K, Fauler G, Moser VA, Greimel T, Zobl J, et al. Neonatal sepsis leads to early rise of rare serum bile acid tauro-omega-muricholic acid (TOMCA). Pediatr Res. 2018.
43. Zollner G, Trauner M. Mechanisms of cholestasis. Clinics in liver disease. 2008;12(1):1-26, vii.
44. Setchell KD, Suchy FJ, Welsh MB, Zimmer-Nechemias L, Heubi J, Balistreri WF. Delta 4-3-oxosteroid 5 beta-reductase deficiency described in identical twins with neonatal hepatitis. A new inborn error in bile acid synthesis. The Journal of clinical investigation. 1988;82(6):2148-57.
45. Cheng JB, Jacquemin E, Gerhardt M, Nazer H, Cresteil D, Heubi JE, et al. Molecular genetics of 3beta-hydroxy-Delta5-C27-steroid oxidoreductase deficiency in 16 patients with loss of bile acid synthesis and liver disease. J Clin Endocrinol Metab. 2003;88(4):1833-41.
46. Fawaz R, Baumann U, Ekong U, Fischler B, Hadzic N, Mack CL, et al. Guideline for the Evaluation of Cholestatic Jaundice in Infants: Joint Recommendations of the North American Society for Pediatric Gastroenterology, Hepatology, and Nutrition and the European Society for Pediatric Gastroenterology, Hepatology, and Nutrition. J Pediatr Gastroenterol Nutr. 2017;64(1):154-68.
47. Mittal V, Saxena AK, Sodhi KS, Thapa BR, Rao KL, Das A, et al. Role of abdominal sonography in the preoperative diagnosis of extrahepatic biliary atresia in infants younger than 90 days. AJR Am J Roentgenol. 2011;196(4):W438-45.
48. Morotti RA, Jain D. Pediatric Cholestatic Disorders: Approach to Pathologic Diagnosis. Surg Pathol Clin. 2013;6(2):205-25.
49. Baumann U, Ure B. Biliary atresia. Clin Res Hepatol Gastroenterol. 2012;36(3):257-9.
50. Mieli-Vergani G, Vergani D, Baumann U, Czubkowski P, Debray D, Dezsofi A, et al. Diagnosis and Management of Pediatric Autoimmune Liver Disease: ESPGHAN Hepatology Committee Position Statement. J Pediatr Gastroenterol Nutr. 2018;66(2):345-60.
51. Hirschfield GM, Dyson JK, Alexander GJM, Chapman MH, Collier J, Hubscher S, et al. The British Society of Gastroenterology/UK-PBC primary biliary cholangitis treatment and management guidelines. Gut. 2018;67(9):1568-94.
52. Chapman MH, Thorburn D, Hirschfield GM, Webster GGJ, Rushbrook SM, Alexander G, et al. British Society of Gastroenterology and UK-PSC guidelines for the diagnosis and management of primary sclerosing cholangitis. Gut. 2019;68(8):1356-78.
53. Geenes V, Williamson C. Intrahepatic cholestasis of pregnancy. World journal of gastroenterology. 2009;15(17):2049-66.
54. Fargo MV, Grogan SP, Saguil A. Evaluation of Jaundice in Adults. Am Fam Physician. 2017;95(3):164-8.
55. Devarbhavi H. An Update on Drug-induced Liver Injury. J Clin Exp Hepatol. 2012;2(3):247-59.
56. Sakiani S, Kleiner DE, Heller T, Koh C. Hepatic Manifestations of Cystic Fibrosis. Clinics in liver disease. 2019;23(2):263-77.
57. van der Feen C, van der Doef HP, van der Ent CK, Houwen RH. Ursodeoxycholic acid treatment is associated with improvement of liver stiffness in cystic fibrosis patients. J Cyst Fibros. 2016;15(6):834-8.
58. de Caestecker JS, Jazrawi RP, Petroni ML, Northfield TC. Ursodeoxycholic acid in chronic liver disease. Gut. 1991;32(9):1061-5.

59. Hempfling W, Dilger K, Beuers U. Systematic review: ursodeoxycholic acid--adverse effects and drug interactions. Alimentary pharmacology & therapeutics. 2003;18(10):963-72.
60. Lindor KD, Kowdley KV, Luketic VA, Harrison ME, McCashland T, Befeler AS, et al. High-dose ursodeoxycholic acid for the treatment of primary sclerosing cholangitis. Hepatology (Baltimore, Md). 2009;50(3):808-14.
61. Fickert P, Zollner G, Fuchsbichler A, Stumptner C, Weiglein AH, Lammert F, et al. Ursodeoxycholic acid aggravates bile infarcts in bile duct-ligated and Mdr2 knockout mice via disruption of cholangioles. Gastroenterology. 2002;123(4):1238-51.
62. Fickert P, Pollheimer MJ, Silbert D, Moustafa T, Halilbasic E, Krones E, et al. Differential effects of norUDCA and UDCA in obstructive cholestasis in mice. Journal of hepatology. 2013;58(6):1201-8.
63. Zhu C, Boucheron N, Muller AC, Majek P, Claudel T, Halilbasic E, et al. 24-Norursodeoxycholic acid reshapes immunometabolism in CD8(+) T cells and alleviates hepatic inflammation. Journal of hepatology. 2021;75(5):1164-76.
64. Fickert P, Hirschfield GM, Denk G, Marschall HU, Altorjay I, Farkkila M, et al. norUrsodeoxycholic acid improves cholestasis in primary sclerosing cholangitis. Journal of hepatology. 2017;67(3):549-58.
65. Halilbasic E, Steinacher D, Trauner M. Nor-Ursodeoxycholic Acid as a Novel Therapeutic Approach for Cholestatic and Metabolic Liver Diseases. Digestive diseases (Basel, Switzerland). 2017;35(3):288-92.
66. Prokopic M, Beuers U. Management of primary sclerosing cholangitis and its complications: an algorithmic approach. Hepatol Int. 2021;15(1):6-20.
67. Kowdley KV, Vuppalanchi R, Levy C, Floreani A, Andreone P, LaRusso NF, et al. A randomized, placebo-controlled, phase II study of obeticholic acid for primary sclerosing cholangitis. Journal of hepatology. 2020;73(1):94-101.
68. Scharf RE. Platelet Signaling in Primary Haemostasis and Arterial Thrombus Formation: Part 1. Hamostaseologie. 2018;38(4):203-10.
69. Broos K, Feys HB, De Meyer SF, Vanhoorelbeke K, Deckmyn H. Platelets at work in primary hemostasis. Blood Rev. 2011;25(4):155-67.
70. Berndt MC, Metharom P, Andrews RK. Primary haemostasis: newer insights. Haemophilia. 2014;20 Suppl 4:15-22.
71. De Meyer SF, Deckmyn H, Vanhoorelbeke K. von Willebrand factor to the rescue. Blood. 2009;113(21):5049-57.
72. Scharf RE. Platelet Signaling in Primary Haemostasis and Arterial Thrombus Formation: Part 2. Hamostaseologie. 2018;38(4):211-22.
73. Davie EW, Ratnoff OD. Waterfall Sequence for Intrinsic Blood Clotting. Science. 1964;145(3638):1310-2.
74. Macfarlane RG. An Enzyme Cascade in the Blood Clotting Mechanism, and Its Function as a Biochemical Amplifier. Nature. 1964;202:498-9.
75. Mackman N. The many faces of tissue factor. J Thromb Haemost. 2009;7 Suppl 1:136-9.
76. Furie B, Furie BC. Thrombus formation in vivo. The Journal of clinical investigation. 2005;115(12):3355-62.
77. Hoffman M. Remodeling the blood coagulation cascade. J Thromb Thrombolysis. 2003;16(1-2):17-20.
78. Hoffman M, Monroe DM, Roberts HR. Cellular interactions in hemostasis. Haemostasis. 1996;26 Suppl 1:12-6.
79. Monroe DM, Hoffman M. What does it take to make the perfect clot? Arterioscler Thromb Vasc Biol. 2006;26(1):41-8.
80. De Caterina R, Husted S, Wallentin L, Andreotti F, Arnesen H, Bachmann F, et al. General mechanisms of coagulation and targets of anticoagulants (Section I). Position Paper of the ESC Working Group on Thrombosis--Task Force on Anticoagulants in Heart Disease. Thromb Haemost. 2013;109(4):569-79.
81. Hoffman M, Monroe DM, 3rd. A cell-based model of hemostasis. Thromb Haemost. 2001;85(6):958-65.

82. Becker RC. Cell-based models of coagulation: a paradigm in evolution. J Thromb Thrombolysis. 2005;20(1):65-8.
83. Spangenberg P, Heller R, Wagner C, Till U. Localization of phosphatidylethanolamine in the plasma membrane of diamide-treated human blood platelets. Biomed Biochim Acta. 1985;44(9):1335-41.
84. Monroe DM, Hoffman M, Roberts HR. Platelets and thrombin generation. Arterioscler Thromb Vasc Biol. 2002;22(9):1381-9.
85. Diaz-Ricart M, Estebanell E, Lozano M, Aznar-Salatti J, White JG, Ordinas A, et al. Thrombin facilitates primary platelet adhesion onto vascular surfaces in the absence of plasma adhesive proteins: studies under flow conditions. Haematologica. 2000;85(3):280-8.
86. Monroe DM, Hoffman M, Roberts HR. Transmission of a procoagulant signal from tissue factor-bearing cell to platelets. Blood Coagul Fibrinolysis. 1996;7(4):459-64.
87. Rao LV, Kothari H, Pendurthi UR. Tissue factor encryption and decryption: facts and controversies. Thromb Res. 2012;129 Suppl 2:S13-7.
88. Chen VM, Hogg PJ. Encryption and decryption of tissue factor. J Thromb Haemost. 2013;11 Suppl 1:277-84.
89. Rao LV, Pendurthi UR. Regulation of tissue factor coagulant activity on cell surfaces. J Thromb Haemost. 2012;10(11):2242-53.
90. Versteeg HH, Ruf W. Tissue factor coagulant function is enhanced by protein-disulfide isomerase independent of oxidoreductase activity. The Journal of biological chemistry. 2007;282(35):25416-24.
91. Wang J, Pendurthi UR, Rao LVM. Acid sphingomyelinase plays a critical role in LPS- and cytokine-induced tissue factor procoagulant activity. Blood. 2019;134(7):645-55.
92. Wang J, Pendurthi UR, Rao LVM. Sphingomyelin encrypts tissue factor: ATP-induced activation of A-SMase leads to tissue factor decryption and microvesicle shedding. Blood Adv. 2017;1(13):849-62.
93. Crawley J, Lupu F, Westmuckett AD, Severs NJ, Kakkar VV, Lupu C. Expression, localization, and activity of tissue factor pathway inhibitor in normal and atherosclerotic human vessels. Arterioscler Thromb Vasc Biol. 2000;20(5):1362-73.
94. Ellery PE, Adams MJ. Tissue factor pathway inhibitor: then and now. Seminars in thrombosis and hemostasis. 2014;40(8):881-6.
95. Adams M. Tissue factor pathway inhibitor: new insights into an old inhibitor. Seminars in thrombosis and hemostasis. 2012;38(2):129-34.
96. Olson ST, Richard B, Izaguirre G, Schedin-Weiss S, Gettins PG. Molecular mechanisms of antithrombin-heparin regulation of blood clotting proteinases. A paradigm for understanding proteinase regulation by serpin family protein proteinase inhibitors. Biochimie. 2010;92(11):1587-96.
97. Rezaie AR, Giri H. Anticoagulant and signaling functions of antithrombin. J Thromb Haemost. 2020;18(12):3142-53.
98. Shahzad K, Kohli S, Al-Dabet MM, Isermann B. Cell biology of activated protein C. Curr Opin Hematol. 2019;26(1):41-50.
99. Griffin JH, Fernandez JA, Gale AJ, Mosnier LO. Activated protein C. J Thromb Haemost. 2007;5 Suppl 1:73-80.
100. Dahlback B, Villoutreix BO. Regulation of blood coagulation by the protein C anticoagulant pathway: novel insights into structure-function relationships and molecular recognition. Arterioscler Thromb Vasc Biol. 2005;25(7):1311-20.
101. Poisson J, Lemoinne S, Boulanger C, Durand F, Moreau R, Valla D, et al. Liver sinusoidal endothelial cells: Physiology and role in liver diseases. Journal of hepatology. 2017;66(1):212-27.
102. Kopec AK, Luyendyk JP. Role of Fibrin(ogen) in Progression of Liver Disease: Guilt by Association? Seminars in thrombosis and hemostasis. 2016;42(4):397-407.
103. Kopec AK, Joshi N, Luyendyk JP. Role of hemostatic factors in hepatic injury and disease: animal models de-liver. J Thromb Haemost. 2016;14(7):1337-49.

104. Yoshida S, Ikenaga N, Liu SB, Peng ZW, Chung J, Sverdlov DY, et al. Extrahepatic platelet-derived growth factor-beta, delivered by platelets, promotes activation of hepatic stellate cells and biliary fibrosis in mice. Gastroenterology. 2014;147(6):1378-92.
105. Joshi N, Kopec AK, O'Brien KM, Towery KL, Cline-Fedewa H, Williams KJ, et al. Coagulation-driven platelet activation reduces cholestatic liver injury and fibrosis in mice. J Thromb Haemost. 2015;13(1):57-71.
106. Sullivan BP, Weinreb PH, Violette SM, Luyendyk JP. The coagulation system contributes to alphaVbeta6 integrin expression and liver fibrosis induced by cholestasis. Am J Pathol. 2010;177(6):2837-49.
107. Baker K, Joshi N, Cline-Fedewa H, Luyendyk JP. Decryption of Hepatocyte Tissue Factor Procoagulant Activity by Bile Acids Requires Non-apoptotic Phosphatidylserine Externalization. Research and Practice in Thrombosis and Haemostasis. 2017;1(S1).
108. Baker KS, Kopec AK, Pant A, Poole LG, Cline-Fedewa H, Ivkovich D, et al. Direct Amplification of Tissue Factor:Factor VIIa Procoagulant Activity by Bile Acids Drives Intrahepatic Coagulation. Arterioscler Thromb Vasc Biol. 2019;39(10):2038-48.
109. Donato MT, Tolosa L, Gomez-Lechon MJ. Culture and Functional Characterization of Human Hepatoma HepG2 Cells. Methods Mol Biol. 2015;1250:77-93.
110. Cvirn G, Waha J, Ledinski G, Schlagenhauf A, Leschnik B, Koestenberger M, et al. Bed rest does not induce hypercoagulability. Eur J Clin Invest. 2015;45(1):63-9.
111. Pfaffl MW. A new mathematical model for relative quantification in real-time RT-PCR. Nucleic Acids Res. 2001;29(9):e45.
112. Greimel T, Jahnel J, Pohl S, Strini T, Tischitz M, Meier-Allard N, et al. Bile acid-induced tissue factor activity in hepatocytes correlates with activation of farnesoid X receptor. Lab Invest. 2021;101(10):1394-402.
113. Denson LA, Sturm E, Echevarria W, Zimmerman TL, Makishima M, Mangelsdorf DJ, et al. The orphan nuclear receptor, shp, mediates bile acid-induced inhibition of the rat bile acid transporter, ntcp. Gastroenterology. 2001;121(1):140-7.
114. Boyer JL, Hagenbuch B, Ananthanarayanan M, Suchy F, Stieger B, Meier PJ. Phylogenic and ontogenic expression of hepatocellular bile acid transport. Proceedings of the National Academy of Sciences of the United States of America. 1993;90(2):435-8.
115. Panzitt K, Wagner M. FXR in liver physiology: Multiple faces to regulate liver metabolism. Biochim Biophys Acta Mol Basis Dis. 2021;1867(7):166133.
116. Tamesue N, Juniper K, Jr. Concentrations of bile salts at the critical micellar concentration of human gall bladder bile. Gastroenterology. 1967;52(3):473-9.
117. Pyrshev KA, Klymchenko AS, Csucs G, Demchenko AP. Apoptosis and eryptosis: Striking differences on biomembrane level. Biochim Biophys Acta Biomembr. 2018;1860(6):1362-71.
118. Wang J, Pendurthi UR, Yi G, Rao LVM. SARS-CoV-2 infection induces the activation of tissue factor-mediated coagulation via activation of acid sphingomyelinase. Blood. 2021;138(4):344-9.
119. Zhao M, Pan W, Shi RZ, Bai YP, You BY, Zhang K, et al. Acid Sphingomyelinase Mediates Oxidized-LDL Induced Apoptosis in Macrophage via Endoplasmic Reticulum Stress. J Atheroscler Thromb. 2016;23(9):1111-25.
120. Maiers JL, Malhi H. Endoplasmic Reticulum Stress in Metabolic Liver Diseases and Hepatic Fibrosis. Semin Liver Dis. 2019;39(2):235-48.
121. Koo JH, Lee HJ, Kim W, Kim SG. Endoplasmic Reticulum Stress in Hepatic Stellate Cells Promotes Liver Fibrosis via PERK-Mediated Degradation of HNRNPA1 and Up-regulation of SMAD2. Gastroenterology. 2016;150(1):181-93 e8.
122. Wang D, Wei Y, Pagliassotti MJ. Saturated fatty acids promote endoplasmic reticulum stress and liver injury in rats with hepatic steatosis. Endocrinology. 2006;147(2):943-51.
123. Cremers CM, Knoefler D, Vitvitsky V, Banerjee R, Jakob U. Bile salts act as effective protein-unfolding agents and instigators of disulfide stress in vivo. Proceedings of

the National Academy of Sciences of the United States of America. 2014;111(16):E1610-9.
124. Han CY, Rho HS, Kim A, Kim TH, Jang K, Jun DW, et al. FXR Inhibits Endoplasmic Reticulum Stress-Induced NLRP3 Inflammasome in Hepatocytes and Ameliorates Liver Injury. Cell Rep. 2018;24(11):2985-99.
125. Liu X, Guo GL, Kong B, Hilburn DB, Hubchak SC, Park S, et al. Farnesoid X receptor signaling activates the hepatic X-box binding protein 1 pathway in vitro and in mice. Hepatology (Baltimore, Md). 2018;68(1):304-16.
126. Wang S, Chen Z, Lam V, Han J, Hassler J, Finck BN, et al. IRE1alpha-XBP1s induces PDI expression to increase MTP activity for hepatic VLDL assembly and lipid homeostasis. Cell Metab. 2012;16(4):473-86.
127. Terada K, Manchikalapudi P, Noiva R, Jauregui HO, Stockert RJ, Schilsky ML. Secretion, surface localization, turnover, and steady state expression of protein disulfide isomerase in rat hepatocytes. The Journal of biological chemistry. 1995;270(35):20410-6.
128. Versteeg HH, Ruf W. Thiol pathways in the regulation of tissue factor prothrombotic activity. Curr Opin Hematol. 2011;18(5):343-8.
129. Raturi A, Ruf W. Effect of protein disulfide isomerase chaperone activity inhibition on tissue factor activity. J Thromb Haemost. 2010;8(8):1863-5.
130. Langer F, Ruf W. Synergies of phosphatidylserine and protein disulfide isomerase in tissue factor activation. Thromb Haemost. 2014;111(4):590-7.
131. Parizek A, Simjak P, Cerny A, Sestinova A, Zdenkova A, Hill M, et al. Efficacy and safety of ursodeoxycholic acid in patients with intrahepatic cholestasis of pregnancy. Ann Hepatol. 2016;15(5):757-61.
132. Mueller M, Thorell A, Claudel T, Jha P, Koefeler H, Lackner C, et al. Ursodeoxycholic acid exerts farnesoid X receptor-antagonistic effects on bile acid and lipid metabolism in morbid obesity. Journal of hepatology. 2015;62(6):1398-404.
133. Danese S, Papa A, Saibeni S, Repici A, Malesci A, Vecchi M. Inflammation and coagulation in inflammatory bowel disease: The clot thickens. Am J Gastroenterol. 2007;102(1):174-86.
134. Danese S, de la Motte C, Sturm A, Vogel JD, West GA, Strong SA, et al. Platelets trigger a CD40-dependent inflammatory response in the microvasculature of inflammatory bowel disease patients. Gastroenterology. 2003;124(5):1249-64.
135. Danese S. Inflammation and the mucosal microcirculation in inflammatory bowel disease: the ebb and flow. Current opinion in gastroenterology. 2007;23(4):384-9.
136. Woolbright BL, Jaeschke H. Inflammation and Cell Death During Cholestasis: The Evolving Role of Bile Acids. Gene Expr. 2019;19(3):215-28.
137. Shoda J, Mahara R, Osuga T, Tohma M, Ohnishi S, Miyazaki H, et al. Similarity of unusual bile acids in human umbilical cord blood and amniotic fluid from newborns and in sera and urine from adult patients with cholestatic liver diseases. J Lipid Res. 1988;29(7):847-58.
138. Meinel K, Szabo D, Dezsofi A, Pohl S, Strini T, Greimel T, et al. The Covert Surge: Murine Bile Acid Levels Are Associated With Pruritus in Pediatric Autoimmune Sclerosing Cholangitis. Front Pediatr. 2022;10:903360.